uOttawa

L'Université canadienne
Canada's university

FACULTÉ DES ÉTUDES SUPÉRIEURES ET POSTOCTORALES

uOttawa

L'Université canadienne
Canada's university

FACULTY OF GRADUATE AND POSDOCTORAL STUDIES

Julie Warrington
AUTEUR DE LA THÈSE / AUTHOR OF THESIS

M.A.Sc. (Biology)
GRADE / DEGREE

Department of Biology
FACULTÉ, ÉCOLE, DÉPARTEMENT / FACULTY, SCHOOL, DEPARTMENT

Chirping *in vitro*: Cellular mechanisms of electrocommunication signal generation in the pacemaker nucleus of *Apteronotus leptorhynchus*

TITRE DE LA THÈSE / TITLE OF THESIS

Dr. J. Lewis
DIRECTEUR (DIRECTRICE) DE LA THÈSE / THESIS SUPERVISOR

CO-DIRECTEUR (CO-DIRECTRICE) DE LA THÈSE / THESIS CO-SUPERVISOR

EXAMINATEURS (EXAMINATRICES) DE LA THÈSE / THESIS EXAMINERS

Dr. J. Dawson

Dr. V. Trudeau

Dr. K. Gilmour

Gary W. Slater
Le Doyen de la Faculté des études supérieures et postdoctorales / Dean of the Faculty of Graduate and Postdoctoral Studies

Chirping *in vitro*: Cellular mechanisms of electrocommunication signal generation in the pacemaker nucleus of *Apteronotus leptorhynchus*

Julie Warrington

Thesis submitted to the
Faculty of Graduate and Postdoctoral Studies
University of Ottawa
in partial fulfillment of the requirements for the degree of

Masters of Science in Biology

Ottawa-Carleton Institute of Biology

Thèse soumise à
la Faculté des Études Supérieures et Postdoctorales
Université d'Ottawa
En vue de l'obtention de la

Maitrîse en Science Biologique

L'Institut de Biologie d'Ottawa-Carleton

Your file Votre référence
ISBN: 978-0-494-46503-5
Our file Notre référence
ISBN: 978-0-494-46503-5

Table of contents

Section	*Page*
List of figures	iv
List of abbreviations	v
Abstract (English)	vi
Résumé (Français)	vii
Acknowledgements	viii
Chapter 1: Introduction	1
1.1 Weakly electric fish: Integrating brain and behaviour	2
1.2 What is a biological oscillator?	7
1.3 *Apteronotus leptorhynchus*: A model system for biological oscillation	10
1.4 Neural control of the EOD: The Pacemaker nucleus (Pn)	11
1.5 Approaches to studying the pacemaker nucleus of *Apteronotus leptorhynchus in vitro*	14
1.5.1 The Pn *in vitro*	14
1.5.2 The Pn *in vitro* in the context of chirping	15
1.6 Chirp-generating mechanisms in the Pn	16
1.7 Cellular mechanisms of chirp generation in the Pn	18
Chapter 2: Chirping *in vitro*	23
2.1 Materials and Methods	24
2.1.1 Fish	24
2.1.2 *In vitro* tissue preparation	24
2.1.3 Neurobiotin application for anterograde transport	26
2.1.4 Processing and visualization	26
2.1.5 Recording and stimulation protocols	27
2.1.6 Pharmacological agents	27
2.1.7 Analysis	28
2.2 Results	30
2.2.1 Immunohistochemistry: Physical characteristics of the Pn	30
2.2.1a Axonal transport of Neurobiotin	30
2.2.1b Topography of pacemaker nucleus cell types	31

2.2.2 Electrophysiology: Pn response to electrical stimulation of afferents 33
2.2.2a Phase response curves 34
2.2.2b Amplitude 36
2.2.2c Relative phase lag 37
2.2.2d Glutamate pharmacology 38

2.3 Discussion 40
2.3.1 Overview 40
2.3.2 Quantification of chirp-like responses in Pn: Single cell responses 42
2.3.3 Quantification of phase lags between paired cells 43
2.3.4 Creating chirps in the Pn: Desynchronization 45
2.3.5 Generating chirps in the electric organ by desynchronization 47

Chapter 3: Conclusions and Future Directions 64

3.1 General conclusions 65
3.2 Synaptic mechanisms of Pn cell responses 65
3.3 Characterization of the responses of Pn cell types 69
3.4 Characterizing relay cell output 71
3.5 Chirping in the Pn *in vivo* 72

Appendix: Glossary of terms 73

Bibliography 77

List of Figures

Number	*Description*	*Page*
1.1	Properties of the electric organ discharge, chirps and chirp generation circuitry in *Apteronotus sp.*	19
1.2	Schematic of neural pathways of the electrosensory system of wave-type weakly electric fish	21
2.1	Confocal micrographs of pacemaker nucleus tissue stained for fluorescence	48
2.2	Schematic diagram of the distribution of cell types in the pacemaker nucleus.	50
2.3	Visual description of action potential amplitude, cycle duration and relative phase lag measurements	52
2.4	Phase response curves for first three post-stimulus cycles	54
2.5	Phase response curves for first three post-stimulus cycles in an individual cell pair	56
2.6	Relative amplitude of first ten post-stimulus cycles	58
2.7	Relative phase lag of first ten post-stimulus cycles	60
2.8	Visual description of chirp-generation mechanisms in the pacemaker nucleus	62

List of abbreviations

ACSF	Artificial cerebrospinal fluid
AFR	Abrupt frequency rise
AMPA	alpha-amino-3-hydroxy-5-methyl-4-isoxazolepropionic acid
AP-5	(2*R*)-amino-5-phosphonopentanoate (NMDA-type glutamate receptor antagonist)
Baclofen	GABA-B Receptor agonist
CLX	Carbenoxolone
CNQX	6-cyano-7-nitroquinoxaline-2,3-dione (AMPA/kainate-type glutamate receptor antagonist)
CV	Coefficient of variation
ELL	Electrosensory lateral line lobe
EOD	Electric organ discharge
F	Frequency of oscillation
GABA	Gamma-aminobutyric acid
JAR	Jamming avoidance response
LTFE	Long-term frequency elevation
MS-222	Tricane Methanosulfate
Muscimol	GABA-A Receptor agonist
nE	Nucleus electrosensorius
NMDA	N-methyl-D-aspartic acid
nP	Nucleus praeeminentialis
Pn	Pacemaker nucleus
φ (Phi)	Phase of oscillation
PRC	Phase reponse curve
PPn	Prepacemaker nucleus
PPnC	Segment of the PPn responsible for eliciting chirping
PPnG	Segment of the PPn responsible for eliciting long-term frequency changes
SAN	Sinoatrial node
SCN	Suprachiasmatic nucleus
SPPn	Sublemniscal prepacemaker nucleus
θ_s (Theta)	Phase at which stimulus occurs; Phase of stimulation
T	Cycle period
t	Cycle time
V	Cycle amplitude

Abstract

The pacemaker nucleus (Pn) of the weakly electric brown ghost knifefish (*Apteronotus leptorhynchus*) contains a network of intrinsically oscillating electrically-coupled cells. The oscillation frequency of the Pn is directly correlated with the frequency of firing of the electric organ discharge (EOD), and is responsible for the generation of modulations of the EOD under behavioral control. One such behavioral modulation of the EOD called "chirping" involves a rapid (~15 ms) acceleration of the EOD that is observed during social interactions. Though the production of chirping in the Pn has previously been investigated (Dye 1988), a thorough quantification of the mechanism by which chirp generation in the Pn is accomplished has been lacking. In my study, I have sought to determine the primary mechanism by which the Pn generates chirping. I have used *in vitro* stimulation of the Pn using brief current pulses (100 μs, 500 μA) applied across the axons leading to the Pn. A thorough quantification of Pn cell responses revealed that stimulation caused randomized firing rate acceleration, significant amplitude decreases and transient and randomized changes in the phase relationships between pairs of cells. The phase relationship response was eliminated with bath application of an AMPA-type glutamate receptor antagonsist but not with an NMDA-type antagonist, indicating that this response is attributable to chirping inputs from the PPnC, which is responsible for eliciting chirping *in vivo*. Due to the randomized nature of observed accelerations and phase relationship changes in the Pn, I have concluded that the the primary mechanism by which chirping is generated in the Pn involves a transient desynchronization of cell firing and not a synchronous change in firing frequency.

Résumé

Le noyau pacemaker (Pn) du poisson-couteau brun (*Apteronotus leptorhynchus*) est formé d'un réseau de cellules électriquement couplées qui oscillent intrinsèquement à une fréquence corrélée directement à la fréquence de décharge de leur organe électrique (EOD). Le Pn est responsable de la génération des modulations de l'EOD sous le contrôle comportemental. Une des modulations de l'EOD nommée « chirping » implique une accélération rapide (~15 ms) de la fréquence de l'EOD observée pendant les interactions sociales. Malgré les études précédentes sur la génération des chirps dans le Pn (Dye 1988), il nous manque une quantification rigoureuse de ce mécanisme. Durant mes études, j'ai cherché à mieux comprendre le mécanisme primaire responsable de la génération des chirps dans le Pn : une accélération synchrone ou un désynchronisation de la décharge des cellules du Pn. J'ai utilisé une stimulation bipolaire *in vitro* d'impulsions brèves de courant (100 μs, 500 μA) appliquées à travers les axones menant au Pn. Une quantification rigoureuse des réponses cellulaires du Pn indique que la stimulation a causé des accélérations de décharges aléatoires, des diminutions significatives d'amplitude et des changements transitoires et aléatoires dans les rapports de phase rélative entre paires de cellules. Ce changement dans les rapports de phase à été éliminée par l'application de CNQX (20 μM) mais pas après application de AP-5 (50 μM), ce qui implique les axones venant du PPnC (responsables de la production de chirps) dans la production de cette réponse. En tenant compte la nature aléatoire des accélérations et des changements de rapport de phase, je conclus que le mécanisme de « désynchronisation » est probablement le principal responsable de la génération de chirps dans le Pn.

Acknowledgements

I would like to thank my supervisor, Dr. John Lewis, for introducing me to the amazing world of weakly electric fish, and for being the best teacher and mentor I ever had. I will be forever grateful for having spent the last four of my undergraduate and graduate years being guided by him in a warm and encouraging environment. I am a better scientist, teacher and person for having been his student, and I can only hope to instill the same level of curiosity and love for science in my future students as he has instilled in me.

Thank you to my lab colleagues for helping me with my daily experimental troubles, for sharing the last few years with me and making even the toughest of days more fun. Thank you to Sally Groothuis, Ginette Hupé, Gerri Mileva, Wudu Lado, Daniel Zysman, Michael Ben-Ezra, Emily Creede, Marc Kelly, Gary Marsat, Erik Harvey-Girard and Zhaohong Qin. A special thank you to Sally Groothuis, who helped guide me through the development of many of the methods I used during my experiments.

I am grateful for the advice and guidance of my thesis committee members: Dr. Jeff Dawson, Dr. Leonard Maler and Dr. Vance Trudeau. Thank you for helping me along the path to successfully completing my thesis.

Thank you to the University of Ottawa and to NSERC for funding my studies and my research, and to Dr. Peter Heinermann and Dr. Fabien Avaron for being great supervisors during my terms as a laboratory teaching assistant.

A big thank you goes to my family for their endless love and encouragement. Thank you to my faithful dog Yoshi, who has been my companion and friend for fifteen years. Thank you to my brothers Jeff, Chris and Steve for putting up with a little sister all these years, and to my parents for helping give me the opportunity and the support I needed to grow into a good student and an independent and successful person. A final thank you goes to Guillaume, my fiancé and the love of my life, who is always by my side when I need him.

Chapter 1

Introduction

1.1 Weakly electric fish: Integrating brain and behavior

The strongly electric eel (*Electrophorus electricus*) is only one of many fish species capable of generating electricity. The majority of electric fish species only produce a much weaker and non-harmful electric field. The fish that generate this much weaker field are referred to as "weakly electric" fish. The electric organ discharge (EOD) of weakly electric fish was first described in *Gymnarchus niloticus*, an African species of weakly electric fish (Lissman 1951). Not only did *G. niloticus* produce weakly electric (millivolt range) signals from its electric organ; it also exhibited behavioral responses to external electric fields. It was later discovered that the EOD is used by weakly electric fish to detect objects in their environment, paving the way for the study of a novel sensory modality, the electric sense, which is controlled by the neural pathways of the electrosensory system (Lissmann, 1951, Lissmann and Machin, 1958, Alves-Gomes et al., 1995, Zupanc, 2002).

Weakly electric fish belong to two major independently evolved groups: the Mormyriformes of Africa and Gymnotiformes of South America, which do not share a common EOD-producing ancestor. Within both of these groups are species that emit an EOD as discrete pulses at irregular intervals ('pulse-type' fish), and those that emit an EOD as a wave-like continuous discharge at a regular frequency ('wave-type' fish, see Figure 1.1A) (Hopkins, 1995).

The EOD of both pulse-type and wave-type fish is generated by an electric organ in the tail of the fish, which is driven by a special pacemaker nucleus in the medullary region of the brain. It is for this reason that the study of wave-type weakly

electric fish lends itself well to the study of biological oscillators, since the EOD can be used as a direct behavioral measure of rhythmic activity in the brain (Dye, 1988, Moortgat et al., 1998, Smith, 2006). The brown ghost knifefish *Apteronotus leptorhynchus* is one of the most intensely studied wave-type electric fish species, and is the organism of study for my thesis.

Weakly electric fish exhibit a substantial array of communication and territorial behaviors. Wave-type fish modulate their EOD in characteristic ways, changing their EOD frequency and amplitude under precise control. The shortest of these modulations, lasting tens of milliseconds, is most often referred to as a chirp, and occurs frequently during courtship and aggressive social interactions. In Figure 1.1B, an instantaneous frequency plot of a chirp recorded from a free-swimming *A. leptorhynchus* is shown. Note that the chirp involves an EOD frequency rise of approximately 75 Hz or 9% the baseline frequency of the EOD of the fish, and lasts only ~15-20 ms.

By contrast, longer types of modulations can last from seconds to hours; the most intensely studied being the jamming avoidance response (JAR), which involves an increase or decrease in EOD frequency in one fish in response to the EOD of a nearby fish with a similar frequency (Juranek and Metzner, 1998, Oestreich and Zakon, 2002, Metzner 1993). The factors that decide which of the fish changes its EOD frequency, and in what direction (increase or decrease), varies between species. *Apteronotus leptorhynchus* can only raise its frequency in response to behavioral stimuli, so when two fish of this species with similar frequencies come in close proximity, it is

automatically the fish with the higher EOD that responds with a JAR and raises its frequency (Juranek and Metzner, 1997, Heiligenberg et al., 1996).

To elicit EOD modulations in an experimental setting, fish are traditionally presented with artificial stimuli or playbacks from other fish through electrodes in the tank (Engler and Zupanc, 2001, Zupanc, 2002, Oestreich and Zakon, 2002, and Triefenbach and Zakon, 2003). More recently, studies have been trying to adopt a more natural approach, using interactions with live conspecifics. A more natural setting can be achieved by placing the fish in physical proximity to allow electric interactions but confining them to prevent confounding physical interaction (Zupanc et al., 2006). In their study, Zupanc et al. (2006) found that *A. leptorhynchus* tended to chirp in an "echo response" fashion, where the chirps of one fish immediately followed those of the other fish. They suggested that this "echo response" pattern is a form of communication between the fish. Hupé and Lewis (2008) achieved an even more naturalistic situation by allowing the fish to physically interact while simultaneously recording their electric and physical interactions. Their study focused on correlating physical behaviors in *A. leptorhynchus* with its communication signals, and found that different signal types are produced under different conditions. They found that chirps are produced following periods of low aggression when the fish are far apart, and not during attack behaviors while the fish are in close proximity.

Electric behavior is inherently fascinating, and provides a wealth of opportunity for behavioral studies. Much attention has also been focused on the neural circuits in control EOD generation and the processing of electrosensory signals (Figure 1.2). The electrosensory lateral line lobe (ELL) in the hindbrain receives input from the

electroreceptors on the skin (Mathieson and Maler 1988). The pyramidal neurons of the ELL respond to stimuli received by electrosensory inputs from the skin receptors, responding differentially to communication signals and prey-like stimuli (Fortune, 2006). The information received by ELL is then processed by a feedback pathway in the higher brain centers; the eminentia granularis pars posterior (EGp), nucleus praeeminentialis (nP) and torus (Figure 1.2). Recent work on this feedback pathway has focused on relating ELL pyramidal cell morphology to their ability to cancel redundant feedback inputs (Bastian et al., 2004). Other recent work has undertaken the development of a novel brain slice that preserves the connection between the ELL and the nP, which can be used in future *in vitro* studies to examine the role of the nP in the feedback pathway (Mileva et al., 2008).

Descending control structures such as the prepacemaker nucleus (PPn), subleminiscal prepacemaker nucleus (SPPn) and pacemaker nucleus (Pn) then modulate the neural output received by the electric organ, consequently affecting the production of EOD modulations such as chirps and the JAR (Zupanc and Maler, 1997, Oestreich and Zakon, 2002). Most of the study of these descending control structures has been focused on long-term frequency changes, including the jamming avoidance response, which can last from seconds to hours (Juranek and Metzner, 1998, Oestreich and Zakon, 2002). The much shorter electrocommunication signals, chirps (~15-30 ms duration), have also been studied in these structures *in vitro*, but to a lesser extent (Dye, 1988). Dye (1988) showed that electrical stimulation of afferents to the Pn can produce short-latency frequency and amplitude changes in the oscillation of Pn cells, which are reminiscent of chirping. Juranek and Metzner (1998) characterized differences between

Pn cell reponses *in vivo* to the different pharmacological inputs to Pn (Figures 1.1C and 1.2) from the SPPn and different parts of the PPn. Oestreïch and Zakon (2002) later used long trains of electrical stimuli in isolated pacemaker nuclei *in vitro* to elicit long-term frequency elevations similar to the JAR.

The electrosensory system faces unique sensory challenges. These include extracting three-dimensional information about the surroundings of the fishfrom a two-dimensional image sensed by the electroreceptors on the skin, and filtering relevant behavioral stimuli from the background noise of their environment. Using computational modeling allows researchers to rigorously test the properties of different components of the electrosensory system, to gain a better understanding of how electric fish accomplish these difficult tasks. One of the greatest advantages of a computational approach is that each variable in a system can be manipulated under direct control, with the ultimate goal of understanding the role of each variable in the function of the system. A model of the system can then be developed and its properties related to physiological and behavioral data from research on real fish under experimental conditions.

A few examples in recent research have undertaken computational modeling of the electric field, EOD generation and sensory filtering (Assad, 1997, Caputi, 2004, Kelly et al., 2008). Caputi (2004) described the implementation of various active strategies used in sensory-motor systems for decoding sensory information from patterned neural activity. He discussed decoding solutions to the problem faced by sensory-motor systems when different sensory inputs generate the same neural patterns. These solutions include actively orienting the sensory surface to explore the source of

interesting signals and the tuning of receptors to a self-generated carrier signal, the EOD. Other studies have examined the production of the EOD in a computational context. Assad (1997) created quantitative reconstructions of the generation of the EOD and electrosensory images detected by weakly electric fish. These concepts were later expanded upon by Kelly et al. (2008) among many others (e.g., Caputi and Budelli, 2006), who recreated biophysical models of the interaction of the EODs of pairs of fish. Their model can be used to determine the electrosensory inputs that induce chirping during behavioral studies.

Weakly electric fish and consequently the EOD are also valuable in the context of studying the neural control of biological oscillators.. Overt oscillatory behavior can be directly related to the activity of the relatively simple neural networks responsible for EOD control (Smith, 2006). The neural center responsible for direct descending control of the electric organ is the pacemaker nucleus (Pn). Any changes in the firing of Pn neurons are reflected as changes in the EOD (Zakon, 2002). It is the goal of my thesis to determine the mechanism by which the neurons of the Pn cause the rapid EOD changes observed during chirping.

1.2 What is a biological oscillator?

The study of oscillations crosses a multitude of scientific disciplines, on scales ranging from the atomic to the global. In the life sciences, biological oscillators are of particular interest, since they are vital to the functioning of living beings. They are responsible for many behavioral, physiological and locomotory functions in organisms

ranging from bacteria to higher vertebrates (Friesen and Block, 1984, Glass and Mackey 1988, Indic et al., 2007). The broad scope of biological oscillators available for study allows researchers to make comparisons between similar structures in many different model systems. However, before these comparisons can be made, it is important to provide a definition of biological oscillators.

Organs, tissues and cells that exhibit regular rhythmic activity are termed biological oscillators. One of the most popular models for describing the functioning of biological oscillators is the "integrate and fire model" (Glass and Mackey 1988). In this model, the activity of the oscillator rises to a threshold, triggering a physiological event, such as the generation of an action potential. After the event, the system then relaxes back to a lower threshold and begins to rise towards the higher threshold again. By repeating the action of rising and falling between the two thresholds, the system maintains steady rhythmic activity.

The cycle period of an oscillation is the time taken for one full cycle to occur (ie. the time between peaks or zero-crossings), whereas the phase of an oscillation is a particular point in the cycle (ie. A point between 0 and 1; 0 being the start and 1 being the end of a cycle of duration 1). The study of rhythmic activity in biological oscillators often revolves around examining the cycle period and how the period changes due to physiological or environmental stresses or perturbations. When perturbed, oscillators typically respond by resetting their phase ("phase resetting"), and then gradually return to their baseline rhythmic activity. This change in phase results in a transient change in the duration of the cycle period. A common way to analyse the response of an oscillator to perturbations is to plot a phase-response curve (PRC) (Glass and Mackey

1988). PRCs plot normalized cycle time against the phase of the perturbation, in order to reveal any phase-dependent effects of the perturbation on the cycle period (For examples see Figures 2.4 and 2.5).

Physiological rhythms also exhibit intrinsic irregularities due to "noise" or "chaos" (Glass and Mackey 1988). One of the most common measures of the regularity of oscillatory activity is the coefficient of variation (CV) of the period (CV=SD/mean cycle period); the lower the CV, the more temporally precise the oscillation (Moortgat et al., 1998, Moortgat et al., 2000a).

There are many examples of biological oscillators in the nervous system. One such neural structure is the suprachiasmatic nucleus (SCN); a segment of the mammalian hypothalamus that oscillates on a 24-hour cycle known as the circadian rhythm. The SCN serves as a pacemaker for the circadian sleep-wake cycle in mammals, coordinating the activity of a number of neurological oscillators and endocrinological functions, including balancing sympathetic and parasympathetic output to the peripheral organs (Kalsbeek et al., 2007, Moore, 2007).

Central pattern generators (CPGs) are neural circuits found in both vertebrates and invertebrates that control rhythmic motor activity, including the patterns of muscle activation in respiration and locomotion (McCrea and Rybak, 2008). The relatively simple rules governing the input and output mechanisms of CPGs have made them attractive candidates for studying patterned neural activity. Additionally, their relative simplicity has also allowed them to be used as models for creating locomotion patterns in articulated robots (Ijspeert, 2008).

Other biological oscillators occurring in non-neural tissue are the sinoatrial node (SAN) cells of the heart, and the pancreatic β-cells. These are particularly popular model systems because of their implications for human health. The SAN cells produce spontaneous action potentials that drive the rhythmic contraction of the heart, and also have a role in modulating the cardiac rhythm through the action of neurotransmitters of the autonomic system (Barbuti et al., 2007). In the pancreas, gap-junction coupled islets of β-cells control the release of insulin (Kang et al., 2005, Jonkers et al., 1999, Mears et al., 1995).

1.3 *Apteronotus leptorhynchus*: A model system for biological oscillation

The weakly electric wave-type electric organ discharge (EOD) of the South American fish *Apteronotus leptorhynchus* (brown ghost knifefish), is extremely stable. Their EOD is normally constant at an individual-specific frequency of ~500-1200 Hz, and maintains a very low coefficient of variation (CV) of $2x10^{-4}$, which is among the lowest CVs found in nature (Moortgat et al., 2000a). This stability can, however, be disrupted under behavioral control during stereotyped frequency and amplitude modulations. The most intensely studied of these modulations, called a 'chirp', involves characteristic frequency and amplitude modulations that last between 10 and a few hundred milliseconds (Figures 1.1B and 1.1C). Chirps can be induced in the laboratory through interactions with conspecifics, using playbacks of EOD recordings or signals designed to mimic the EOD (Zupanc, 2002, Oestreich and Zakon, 2002, Zupanc et al., 2006, Hupé and Lewis, 2008). The ability to induce quantifiable

behaviors in *A. leptorhynchus*, combined with the high frequency and temporal precision of its EOD makes brown ghost knifefish attractive candidates for studying biological oscillations and their control.

1.4 Neural control of the EOD: The Pacemaker nucleus (Pn)

The neural network that generates the EOD is relatively simple and well-characterized (Figures 1.1C and 1.2). A cluster of ~150 electrically-coupled cells form the medullary brain structure called the pacemaker nucleus (Pn). The Pn oscillates at the frequency of the EOD, and continues to do so with nearly equal precision when removed from the brain (Moortgat et al., 2000a). There are two main cell types within the Pn: pacemaker cells and relay cells. Pacemaker and relay cells are morphologically distinct, with the relay cells (~70 μm diameter) being approximately twice the size of pacemaker cells (~30 μm). There is a third smaller cell type in the Pn, parvocells (~7-15 μm diameter), which are connected via gap junctions to the pacemaker and relay cells and connect to both cell types with chemical synapses (Smith and Zakon 2000). Their anatomical characteristics have been identified, but the function of parvocells in the Pn remains unclear. Pacemaker cell axons connect to several other cells of both types within the Pn, whereas the axons of the relay cells travel down the spinal cord to synapse onto the electric organ cells and induce behavioral EOD changes. The Pn is an intrinsic biological oscillator, and any modulations in the oscillation of the Pn are manifested as changes in the EOD (Ellis and Szabo, 1980, Elekes and Szabo, 1985, Smith, 1999, Moortgat et al., 2000a, Smith et al., 2000, Zupanc, 2002, Smith, 2006).

Figure 1.1C represents the current consensus on the arrangement of inputs to and within the pacemaker nucleus in wave-type weakly electric fish (Dye et al., 1989, Zupanc and Maler, 1997, Zupanc, 2002, Juranek and Metzner, 1997, Juranek and Metzner, 1998, Smith, 2006). The current model for pacemaker nucleus (Pn) inputs states that the Pn receives glutamatergic inputs from the Prepacemaker nucleus (PPn) and Subleminiscal prepacemaker nucleus (SPPn), which are responsible for behavioral modulations of the EOD (Figures 1.1C and 1.2). These glutamatergic inputs are partially segregated according to the types of EOD modulations they produce, via their connections to the different cell types of the Pn (Figure 1.1C).

Both long-term frequency changes and chirps in A. *leptorhynchus* have been studied *in vivo*, in which Pn cells were recorded during evoked EOD modulations (Dye and Heiligenberg, 1987). This technique has also been used to study frequency modulations in related species *Gymnotus carapo* (Curti et al., 1999, Curti et al., 2006), *Eigenmannia* and *Hypopomus* (Kawasaki and Heiligenberg, 1990, Juranek and Metzner, 1998). In the latter three types of fish, the electric organ is derived from muscle tissue, so complete curarization without the elimination of the EOD is not possible, and instead a residual EOD is recorded under lighter curarization. The electric organ of *A. leptorhynchus* is made of neural tissue, thus their electric organ and consequently the EOD is unaffected in curarized animals.

Kawasaki and Heiligenberg (1990) used a similar *in vivo* preparation to stimulate the PPn of *Hypopomus* and *Eigenmannia* and record from the Pn while applying glutamate receptor blockers. They confirmed results from Dye et al. (1989) showing that NMDA-type glutamatergic inputs are responsible for eliciting long-term

frequency changes, whereas AMPA-type inputs are responsible for eliciting chirping. Recording from animals *in vivo* is useful for observing Pn cell activity during evoked or spontaneous EOD modulations.

Juranek and Metzner (1998) recorded changes in the input resistance of relay and pacemaker cells following selective glutamate stimulation of the PPnC, PPnG and SPPn. The cell type for which input resistance was most strongly affected by stimulating each brain region (PPnC, PPnG or SPPn) was determined to be the target cell type for that region. It was determined that the NMDA-type glutamatergic inputs from a segment of the PPn called the PPnG synapse onto the pacemaker cells, and are responsible for inducing long-term frequency changes. NMDA-type synapses from the SPPn connect to the pacemaker cells, and the inhibition of its inputs elicits the jamming avoidance response (Metzner, 1993, Juranek and Metzner, 1998, Oestreich and Zakon, 2002). Chirps are induced by AMPA-type glutamatergic inputs to the relay cells from the PPn segment called the PPnC. Though the segregation of pharmacological inputs to pacemaker and relay cells has been quantified in *Eigenmannia* (Juranek and Metzner 1998), a similar quantification in other wave-type weakly electric fish such as *A. leptorhynchus* has yet to be performed.

Although Juranek and Metzner (1998) succeeded in showing that glutamatergic inputs from PPnC and PPnG respectively project largely to relay and pacemaker cells, the input resistance changes they observed were not all-or-none for each cell type. Relay cells showed a weak response to stimulation of PPnG, and pacemaker cells showed a weak response to stimulation of PPnC (Figure 8 of Juranek and Metzner, 1998). The two types of behavioral inputs can be mostly segregated pharmacologically,

therefore chirping can be studied essentially in isolation from other types of EOD modulations (Dye et al., 1989, Zupanc and Maler, 1997, Zupanc, 2002, Juranek and Metzner, 1997).

1.5 Approaches to studying the pacemaker nucleus of *Apteronotus leptorhynchus in vitro*

1.5.1 The Pn *in vitro*

In vitro preparations of the Pn provide a more controlled environment under which to test the cellular mechanisms by which these modulations are generated. By isolating the Pn from its descending inputs (Figures 1.1C and 1.2), the precise timing and nature of electrical and chemical inputs to the Pn can be controlled. The chemical environment surrounding the Pn can also be manipulated, by altering ionic concentrations, adding synaptic blockers and other chemicals. The Pn of *A. leptorhynchus* is visible as an ovoid protrusion at the base of the ventral brainstem, making it relatively easy to identify and excise (Dye, 1988). Since it is an intrinsic oscillator, the cells of the Pn will oscillate reliably in synchrony for several hours after it is removed from the brain. The Pn is also removed for *in vitro* studies with part of the surrounding brainstem tissue, to provide support for the Pn cells and to allow stimulation of the afferent axons rostral to the Pn. This preparation has been used for numerous applications in *A. leptorhynchus*, such as examining the effects of steroids on Pn discharge frequency (Meyer, 1984), determining the role of different glutamate

receptor subtypes in the generation of electrocommunication signals (Dye et al., 1989), including determining the role of NMDA receptors in the generation of long-term frequency elevations (Oestreich and Zakon, 2002), and for examining the precision Pn firing (Moortgat et al., 2000a).

1.5.2 The Pn *in vitro* in the context of chirping

The Pn is the neural structure in the electrosensory system immediately before the electric organ (Figure 1.2), and is thought to be the final modulatory center for producing changes in the EOD. It therefore stands to reason that the Pn has been investigated with regards to its role in modulatory behaviors such as chirping. When he stimulated the afferents to the Pn *in vitro* with brief current pulses, Dye (1988) observed several changes in the activity of Pn cells. Stimulation caused a short-latency action potential frequency increase, and accelerations were accompanied by membrane potential depolarizations and decreases in action potential amplitude, which were both dependent on the phase and amplitude of stimulation. Pacemaker and relay cells exhibited different responses to stimulation. Relay cells depolarized and accelerated more than pacemaker cells (later confirmed by Juranek and Metzner, 1998 *in vivo*). Phase lags between the majority of cell pairs changed transiently with stimulation, indicating that the synchrony between those cell pairs was temporarily disrupted by the stimulus.

1.6 Chirp-generating mechanisms in the Pn

Transient frequency increases and amplitude decreases in the EOD are defining characteristics of chirps (Figure 1.1B,C and Zupanc, 2002). Since the firing of the Pn is directly related to EOD output (Zupanc, 2002), the frequency and amplitude changes observed by Dye (1988) at short latency may be implicated in chirp production. The question then arises: What is the mechanism by which the cellular network in the Pn generates chirping?

I propose two mechanisms by which the Pn can generate chirps:

1. Synchronous change: PPn input affects all Pn cells, causing them to simultaneously increase their frequency, and thus causing a net frequency increase.
2. Desynchronization: PPn input causes a fraction of Pn cells to transiently and randomly change their frequency, causing an apparent frequency increase across the network resulting from a loss of synchrony between cells.

The frequency of the Pn is normally extremely precise, and the cells of the Pn are extensively electrically coupled (Moortgat et al., 2000a), intuitively making the synchronous change mechanism possible. However, there are properties of the Pn that would suggest that instead the desynchronization mechanism is the primary mechanism. Though there is some tendency for relay cells to be located in the ventral region of the Pn, there is no clear organization of cells in the Pn (Elekes and Szabo, 1985 and Figure

2.2). For synchronous change to be facilitated, Pn cells would have to receive PPn input simultaneously, which is not easily achievable without spatial organization. Unless there are mechanisms, such as differences in afferent axon width that can compensate for timing differences caused by the lack of spatial organization in the Pn, inputs to Pn cells do not likely arrive simultaneously. Additionally, it has been previously suggested that though stable phase relationships exist between pairs of cells under normal conditions (Dye 1988, Moortgat et al. 2000), these phase relationships can be altered by activating the inputs to the Pn through electrical stimulation (Dye 1988).

A similar desynchronization hypothesis comes from modeling of another oscillating system that is responsible for governingthe circadian rhythm of hamsters. The circadian rhythm is governed by the suprachiasmatic nucleus (SCN), which is made up of a network of electrically coupled oscillating neurons (Indic et al., 2007). When hamsters are exposed to 24-hour dark or 24-hour light, their normal daily routine becomes "phase-split". This means that the behavior set normally governed by the SCN on a 24-hour cycle is split into two 12-hour cycles, essentially doubling the frequency of the oscillation of daily activity. This "phase-splitting" behavior is supported by mathematical modeling. If the tendency of an individual oscillator to maintain its rhythm is strong relative to the coupling strength between oscillators, then it is acceptable to define the net activity of the population by considering the phases of each oscillator, without considering their amplitudes (Indic et al., 2007). In other words, if the tendency of individual oscillators to maintain their rhythm is sufficiently strong relative to their tendency to influence one another, then their amplitudes of oscillation can be considered independently. If this concept applies to the Pn, then when an input

from PPn occurs, the net frequency of the Pn can be defined by the phase of oscillation of each of the affected cells. If the phases are as different from one another as half a period, then the frequency of oscillation of the Pn would be doubled. However, since frequency changes during chirps are only a fraction of the Pn oscillating frequency a small phase shift could be enough to cause a chirp-like net frequency increase.

Evidence that both synchronous change and desynchronization mechanisms may be at work to create chirps comes from studying the effects of stimulating the Pn *in vitro*. In previous *in vitro* studies when afferents to the Pn were stimulated (Dye 1988), most cell pairs exhibited phase lag changes as well as increases in their frequency with stimulation. The responses varied greatly between cell pairs and cell types within the pairs, but this variation was not described quantitatively.

1.7 Cellular mechanisms of chirp generation in the Pn

While there is some support for the desynchronization mechanism as the primary means by which chirps are generated in the Pn, a thorough quantification of these findings is lacking. My thesis aimed to resolve this issue by using a similar *in vitro* stimulation protocol to that of Dye (1988) while recording from pairs of cells in the Pn. The data analysis involved a more thorough phase analysis and larger numbers of cells and cell pairs. This more robust quantification provided an important description of the response of the Pn to PPn inputs, which led to a more complete understanding of how chirps are generated in the Pn.

Figure 1.1. Properties of the electric organ discharge, chirps and chirp generation circuitry in *Apteronotus sp.*

(A) EOD waveform of an *Apteronotus albifrons*, close relative of *Apteronotus leptorhynchus* (adapted from Figure 1.1A of Assad, 1997). (B) Instantaneous frequency of a chirp recorded from an isolated *A. leptorhynchus*. Note that the frequency increase is approximately 75 Hz, or 9% of the baseline EOD frequency of the fish, and the chirp lasts 15-20 ms (adapted from Figure 1 of Hupé and Lewis, 2008). (C) Schematic of the connections between cells of the pacemaker nucleus and its neural inputs. Note that the PPnC, responsible for eliciting chirping, excites the relay cells (R) directly through AMPA-type glutamatergic synapses. Long-term frequency elevations and the jamming avoidance response are initiated through NMDA inputs to the Pn from the PPnG to the pacemaker cells, and from the SPPn to the relay cells. Parvocells (interneurons) have been omitted for the sake of clarity (Modified from Oestreich and Zakon, 2002).

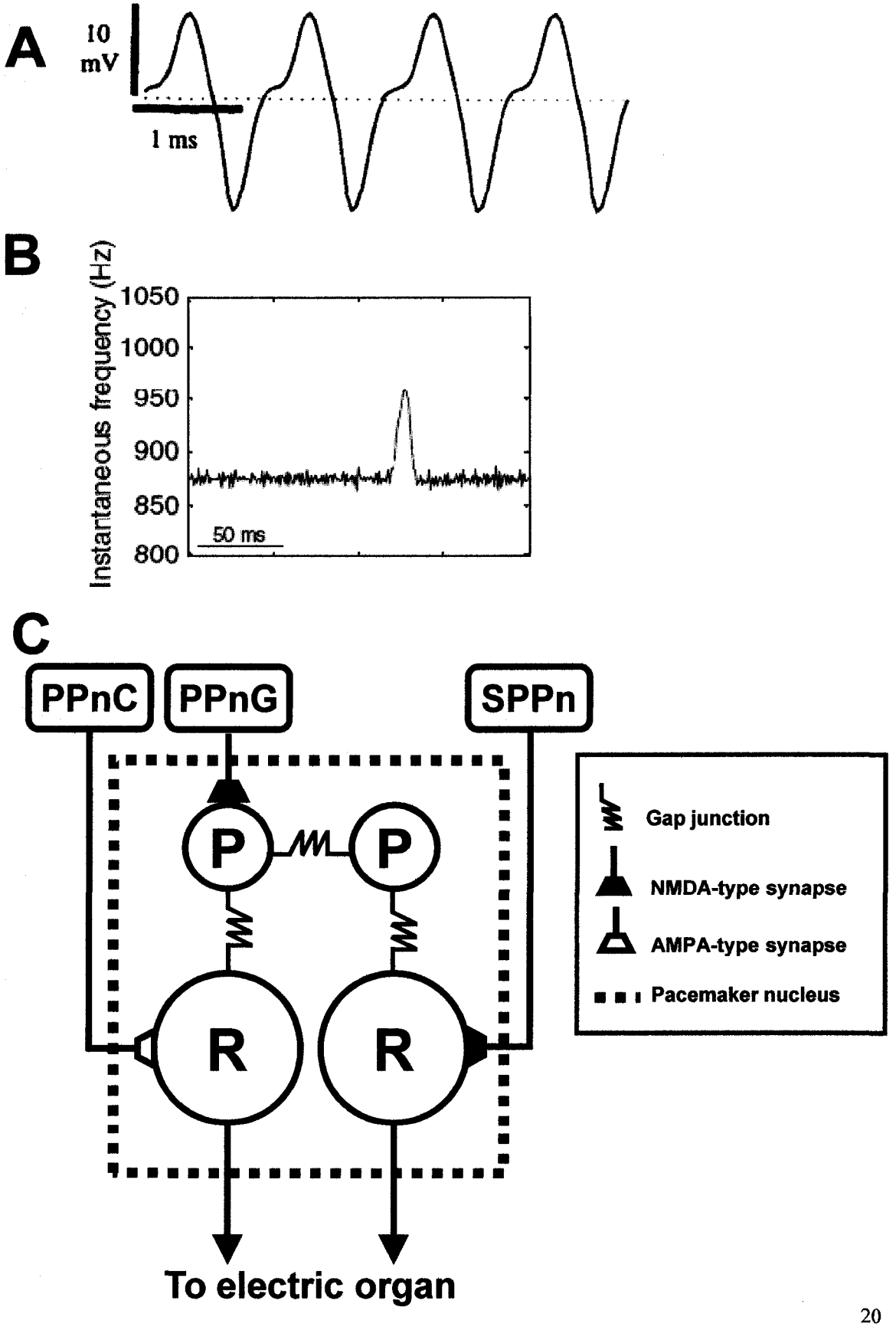
A
10
mV
1 ms
B
Instantaneous frequency (Hz)
1050
1000
950
900
850
800
50 ms
C
PPnC
PPnG
SPPn
P
P
R
R
Gap junction
NMDA-type synapse
AMPA-type synapse
Pacemaker nucleus
To electric organ

Figure 1.2. Schematic of neural pathways of the electrosensory system of wave-type weakly electric fish

Schematic showing the electrosensory pathways in the brain of *Eigenmannia* (modified from Figure 2A of Rose, 2004). Abbreviations represent the electrosensory lateral line lobe (ELL), eminentia granularis pars posterior (EGp), nucleus praeeminentialis (nP), nucleus electrosensorius (nE), sublemniscal prepacemaker nucleus (SPPn), prepacemaker nucleus (PPnG and PPnC) and pacemaker nucleus (Pn). Feedback pathways involved in sensory processing are shown in black, whereas areas shaded in grey are responsible for descending control of EOD output.

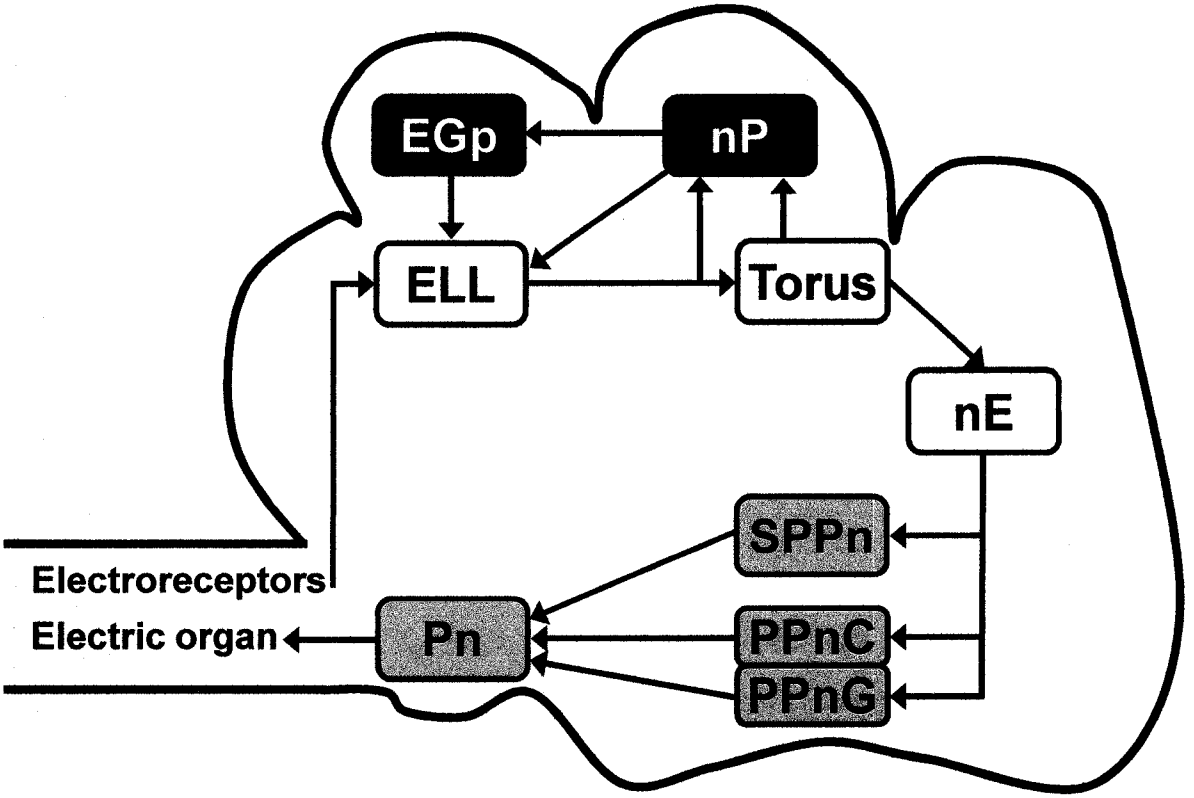
EGp
nP
ELL
Torus
nE
SPPn
Electroreceptors
Electric organ
Pn
PPnC
PPnG

Chapter 2

Chirping *in vitro*

2.1 Materials and Methods

2.1.1 Fish

Adult wild-caught brown ghost knifefish (*Apteronotus leptorhynchus*) were obtained from commercial fish supply companies then housed in flow-through 40 L tanks containing 5-10 individuals. Environmental conditions were held constant with a 12/12 hour light/dark dark cycle with temperature at ~27-28°C, and conductivity at ~150-250 μS. Light cycle lighting was obtained by covering dim fluorescent lighting with green filter paper, and during the dark cycle there was no lighting whatsoever. Fish were fed as many bloodworms as they could eat within 2-3 hours, after which the remaining bloodworms were removed from the tanks. Tanks were aerated by air contact at the surface of the water, and by a small spigot responsible for the inflow of fresh water. All housing and experimental protocols were in accordance with guidelines approved by the Animal Care Committee of the University of Ottawa (BL-229).

2.1.2 *In vitro* tissue preparation

Tissue preparation protocols were similar to those used previously (Ellis and Szabo, 1980, Meyer, 1984, Dye, 1988, Moortgat et al., 2000a, Smith and Zakon, 2000). Fish were briefly anaesthetized with tricane methanosulfate (MS-222, 0.2%) before being transferred to a holder, where their gills were continuously perfused with oxygenated water containing a lighter anaesthetic solution. The brain was dissected and quickly

removed from the fish and transferred to an ice-cold bath of artificial cerebrospinal fluid (ACSF). Salt concentrations (in mM) dissolved in distilled water to make the ACSF were: NaCl (124), $NaHCO_3$ (24), D-glucose (10), KH_2PO_4 (1.25), KCl (2), $MgSO_4$ (2) and $CaCl_2$ (2). The pH of the resulting ACSF was approximately neutral. While holding the anterior part of the brain with forceps, the meninges and blood vessels overlying the pacemaker nucleus and surrounding tissues were carefully removed with fine forceps. This was done in order to facilitate the entry of recording electrodes into the tissue, as well as improving the oxygenation of the tissues through closer contact with the ACSF. The pacemaker nucleus, visible as an ovoid protrusion on the ventral brainstem, was then removed with tissues approximately 1 mm rostral, 0.5 mm caudal and 1 mm dorsal to it, which constituted most of the ventral brainstem. The tissue was immediately transferred to a brain slice chamber which was continuously perfused with room-temperature (~21°C) ACSF from an aerated (95% O_2, 5% CO_2), gravity-fed supply bottle. Preliminary recordings begun after a recovery period of 1 hour, and data collection commenced 0.5-1 hour the initial recovery period, once it was determined by visual inspection that the oscillation of Pn cells had reach acceptable levels of amplitude and frequency stability. Pn slices prepared in this manner maintained stable oscillation approximately for 5-7 hours, after which cellular oscillations were determined by eye to be too unstable to continue experimentation.

2.1.3 Neurobiotin application for anterograde transport

The meninges overlying the Pn were left intact to reduce the amount of labeling resulting from ACSF flow over the surface of the Pn. Three to four neurobiotin crystals were placed on the cut surface of the tissue rostral to the Pn, at the upstream end of ACSF flow. The preparation was then allowed to sit in the perfusion chamber for approximately 5 hours, to allow ample time for the afferent axons to transport the neurobiotin into the Pn.

2.1.4 Processing and visualization

A standard *in vitro* Pn preparation (see section 2.1.2)was fixed overnight (16-18 hours) in 4% paraformaldehyde with 0.5% glutaraldehyde in 0.1 M phosphate buffer (PBS). After fixation, the tissue was sliced into 150 μm sections with a vibratome at room temperature. Sections were then incubated in 1% Triton X-100 in PBS for 4 hours, followed by incubation for 3 hours in the dark in 0.5% Triton X and 1:300 Streptavidin CY-3 in PBS. Tissue sections were then placed onto slides and coverslipped with a 50:50 mixture of glycerol and PBS before being stored at -20°C. Fluorescence images were captured using confocal microscopy and were later adjusted digitally to optimize contrast, brightness and sharpness.

2.1.5 Recording and stimulation protocols

Stimulation protocols were similar to those used by Dye (1988). Bipolar stimuli were delivered through $Ag/AgCl_2$ electrodes, placed rostral of the Pn on each side of the brainstem. Stimuli used were constant current, 100 μs pulses of either 50 to 500 μA. Stimuli were delivered using a Multichannel systems STG1004 stimulator and its associated software (MCS Stimulator). Recordings were made with borosilicate glass micropipette electrodes (60-90 MOhm resistance), which were created using a Sutter Instrument co. P-2000 laser electrode puller and amplified through an Axon Instruments Axoclamp 2B amplifier. Recordings were then converted to digital signals using a National Instruments PCI-6052E data acquisition board, then recorded at a sampling frequency of 10 000 Hz using custom-made MatLab 7 (The Mathworks) software loaded onto an IBM PC. The stimulus was triggered to be delivered 0.2 seconds into a 1-second recording. Single-pulse stimuli were delivered at least 5 seconds apart to prevent the elicitation of long-term frequency changes (Oestreich and Zakon, 2002).

2.1.6 Pharmacological agents

Pharmacological agents were dissolved in oxygenated ACSF and delivered in the same manner as control ACSF (see section 2.1.2). Glutamate receptor antagonists AP-5 (NMDA-type; 50 μM) and CNQX (AMPA-type; 20 μM) (Tocris) were bath applied then washed out with control ACSF. Concentrations are on the higher end of those used

previously in Mormyrid (Zhang and Han, 2007) and guinea pig (Karnup and Stelzer, 2001) brain slice preparations, but lower than those used in zebrafish olfactory bulb (Edwards and Michel, 2003). This moderate concentration was used to help ensure the pharmacological agents fully penetrated the relatively thick (~500 μm) Pn slice.

2.1.7 Analysis

Zero-crossing times and action potential amplitude measurements for the Pn cell oscillations were obtained using custom made MatLab 7 software. Amplitude measurements were recorded as the maximum action potential height from the vertical midline (Figure 2.3A).

For cycle duration and phase measurements, the times of positive zero-crossings were calculated by linear interpolation. The mean amplitude for the entire trial was subtracted to center the signal on zero, and then a linear interpolation between the points immediately below and above zero was used to find the zero-crossing. The cycle duration is the time taken for one full cycle to occur (ie. the time between positive zero-crossings; see Figure 2.3B), whereas the phase is a particular point in the cycle (ie. 0 to 1; 0 being the start and 1 being the end of a single cycle).

The effects of current stimuli on amplitude and relative phase lag values were statistically analyzed in SigmaStat 3.1 (One-way ANOVA on ranks) and Microsoft Excel 2003 (F-tests). One-way ANOVA on ranks was used to determine if there was significant variation in the amplitude or phase lag of the first ten post-stimulus cycles ($P<0.05$). If the ANOVA indicated significant variation, a Tukey multiple paired

comparisons procedure was performed to compare pairs of post-stimulus cycles. F-tests were performed on the relative phase lag values to determine if there was a transient increase in phase lag variability immediately after the stimulus (α=0.01). All trials were considered independently in statistical testing.

2.2 Results

The results section comprised two approaches for characterizing the pacemaker nucleus: anatomical description and electrophysiological testing. The anatomical description involved immunohistological techniques, which were used to reveal the general topography of the Pn. Electrophysiological testing was used to quantify the responses of Pn cells to brief current pulses applied across the afferent axons to the Pn.

2.2.1 Immunohistochemistry: Physical characteristics of the Pn

Previously the topography of pacemaker and relay cells in the Pn of *Apteronotus albifrons* and *Eigenmannia*, other wave-type weakly electric fish species, has been described as lacking spatial organization (Ellis and Szabo 1980). I have confirmed that the Pn of *A. leptorhynchus* similarly lacks spatial organization through immunofluorescence labelling techniques.

2.2.1a Axonal transport of neurobiotin

The axonal anterograde transport of neurobiotin revealed extensive connectivity within the pacemaker nucleus (n=1 preparation). As seen in Figure 2.1A, pacemaker cells, relay cells and cells similar in shape and size to parvocells (Smith et al., 2000) and their processes were observed using this technique. Relay cells found were approximately 60-80 μm, pacemaker cells were 30-50 μm and parvocells were ~15 μm in diameter,

and were distinguished by size alone. The somata of relay cells were never filled with neurobiotin, but occasionally those of pacemaker neurons were filled as seen in Figure 2.1B. The presence of dye within pacemaker cells suggests that either there is some electrical coupling from the afferents to the pacemaker cells, or some of the cellular processes within the Pn were damaged during the dissection, allowing neurobiotin to enter some of the Pn cells in higher concentrations. Clubbed endings of axons within the pacemaker nucleus were observed on both pacemaker and relay cells, as seen in Figures 2.1C and 2.1D respectively. Similar structures were previously observed in pacemaker nucleus preparations, both in *A. leptorhynchus* (Dye, 1988) and in *E. viriscens* (Zupanc and Heiligenberg, 1992).

2.2.1b Topography of pacemaker nucleus cell types

In one pacemaker nucleus preparation, counts of pacemaker and relay cells were obtained by viewing confocal images of the pacemaker nucleus and identifying relay cells and pacemaker cells based on size. A semi-quantitative mapping of the location of pacemaker and relay cells in the Pn is shown in Figure 2.2. Cell counts and locations for three serial 150 μm tissue sections were obtained using 25, 20 and 22 optical confocal sections for Figures 2.2A, 2.2B and 2.2C respectively. Optical sections for the confocal images were equally spaced throughout the depth of each section and encompassed the entire range of the 150 μm. Relay cells (Re) are shown in red as large dots, whereas pacemaker cells (Pm) are shown in blue as small dots in Figures 2.2A through 2.2C. Parvocell locations are not included because only a small number of

parvocells were found, and they were not easily distinguishable. In Figure 2.2A, the location of cells within the section closest to the ventral surface of the pacemaker is shown. In this section, pacemaker and relay cells are dispersed throughout the section, and there were slightly more pacemaker than relay cells (Pm = 13, Re = 9). In the second tissue section, shown in 2.2B, pacemaker cells are more numerous in the central region than relay cells, which are primarily confined to the periphery. In this section, relay cells are somewhat more common than pacemaker cells (Pm=12, Re=16). In the deepest of the three sections (2.2C), pacemaker and relay cells are again dispersed throughout the slice, without any apparent clustering. Pacemaker cells in this region are nearly equal in number to relay cells (Pm = 20, Re = 19). It should also be noted that the overall number of cells in the section deepest within the pacemaker is nearly double that of the section closest to the ventral surface; 39 cells for 2.2C (deep section) and 22 cells for 2.2A (surface section).

In Figure 2.2D counts are shown for five regions within the pacemaker from a dorsoventral perspective. The approximate angle and depth of each slice was taken into account when counts were being made. The number of pacemaker cells in the central region is more than double that of the relay cells. Other regions do not show the same trend; in all other regions relay cells outnumber pacemaker cells. The total counts of relay and pacemaker cells were approximately equal and were 44 and 45 cells, respectively. Given that the Pn contains ~150 cells, and that pacemaker cells and relay cells are present in a ratio of 4:1 (Moortgat et al. 2000), it appears that this technique preferentially sampled relay cells. The large number of relay cells indicates that some of the neurobiotin may have flowed over the Pn and entered the Pn tissue through the

cut axons of the relay cells on the downstream end of the slice. This could have caused an increase in the number of relay cells labelled relative to the number of labeled pacemaker cells.

The pacemaker and relay cells were confirmed to be arranged without spatial organization (Figure 2.2). Therefore for the electrophysiological experiments to follow, cells within the Pn were sampled at random recording locations.

2.2.2 Electrophysiology: Pn response to electrical stimulation of afferents

To reveal the mechanism by which the Pn generates chirping, three features of the response to afferent stimulation are of greatest interest: cycle duration changes, amplitude changes and changes in phase lags between cells (Dye, 1988). Figure 2.3 shows the methods used to calculate amplitude changes (Figure 2.3A), period changes (Figure 2.3B) and changes in phase lags between paired cells (Figure 2.3C). Amplitude, period and phase lag characteristics of Pn cell responses will be examined in electrophysiology data in the following sections. Attempts were made to categorize cells as either relay or pacemaker cells according to waveform shape (Bennett et al. 1967), but this was not possible in many cases when the frequency was relatively high (over ~300-350 Hz). The action potentials of relay cells do not exhibit a gradually depolarizing rising phase, and as such appear asymmetrical when compared to the action potentials of pacemaker cells. In cases where pacemaker and relay cells were discernable by waveform (28 out of 45 total cells), their responses were not consistently

different from one another. Therefore, pacemaker and relay cell responses are treated together unless otherwise stated.

2.2.2a Phase response curves

Brief cycle duration changes in the EOD are characteristic of chirping. Therefore, change in the period of oscillation in Pn cells is one of the responses to examine after stimulating Pn afferents. It was previously shown that bipolar electrical stimulation of Pn afferents caused phase-dependent cycle duration changes (Figure 5C in Dye, 1988). Phase response curves (PRCs) reveal any phase-dependent effects of stimulation, and involve plotting a normalized cycle time (T_x) against the phase of stimulation (Glass and Mackey 1988). For example, if the first post-stimulus cycle (T_1) is plotted, a value of 1 would indicate that the cycle in question is exactly the same duration as that of the pre-stimulus cycle. In other words, its timing has been unaffected by the stimulus. Similarly, if the second cycle following the stimulus (T_2) has a value of 2 then it has not been affected by the stimulus. A value of 0.9 for T1 would indicate a 10% period length decrease (frequency increase or phase advance), whereas a value of 1.1 would indicate a 10% period length increase (frequency decrease or phase delay). If T_2 has a value of 1.9 following a T_1 value of 0.9, then by T_2 the cycle duration has returned to its pre-stimulus value.

When the first three post-stimulus cycles are plotted as a phase response curve (Figure 2.4), the results differ greatly from what was observed by Dye (1988). The 50 μA stimulus caused no phase changes (Figure 2.4A), showing that this stimulus size is

too small to elicit a cycle duration response. However the 500 μA stimulus caused variable cycle duration responses in the population data, tending towards cycle duration decreases (Figure 2.4B). There is a trend of increasing variability towards later stimulus phases in cycle 1, near the rising phase of the action potential (Figure 2.4B, T1). There is also increased variability in the durations of cycles 2 and 3 (T2 and T3) but without any phase dependence. Responses range from no period change to up to ~30% period length decreases, corresponding to changes in frequency of up to ~114 Hz based on a mean frequency of ~342 Hz. The maximal frequency increases observed were somewhat higher than those observed previously (Dye 1988).

When the response of a single cell pair is examined (Figure 2.4C), in which there was one relay cell (filled circles) and one pacemaker cell (empty circles), the responses of the two cells are similar, and do not appear to exhibit an overt trend across stimulus phases. Results nearer to the quasi-sinusoidal dependence of cycle duration on phase observed by Dye (1988) can be obtained using the current experimental data by considering only single cells and using a finer scale (Figure 2.5). When examining a single cell pair there is a trend towards the first cycle being most strongly being affected if the stimulus occurred late in the phase of the oscillation ($0.8<\theta_s<1$), and the second cycle being most strongly affected near the halfway point of the oscillation ($0.3<\theta_s<0.7$). The two cells also exhibit a phase lag response in the second post-stimulus cycle (2.5B), which is visible as a discernible gap between the normalized cycle time values between the two cells where the stimulus occurred near the peak of the oscillation ($0<\theta_s<0.3$).

Though the effects of stimulation appear to be phase dependent if single cell pairs are considered in isolation (Figure 2.5), over a larger number of cells and trials, the variability among cell pairs creates a net effect of randomized cycle duration decreases over the entire population (Figure 2.4B). When multiple individual cell pairs are examined in isolation from one another, the magnitude and nature of the phase dependency is not consistent between cell pairs, between different pacemaker nuclei or within the same pacemaker nucleus (data not shown). The cycle duration changes that I observed therefore do not appear to have a clear phase dependency when the entire cell population is considered. This variability is especially apparent when comparing the effects of the 500 μA stimulus (Figure 2.4B) with those of the 50 μA stimulus (Figure 2.4A). The cycle duration changes observed are slightly larger than those observed by Dye (1988), where he observed ~120 Hz frequency increases in pacemaker nuclei oscillating at ~500-700 Hz, representing cycle duration decrease of ~ 21%.

Cycle duration responses in the population data and in individual cells were only weakly phase-dependent (and variable), therefore all further analyses were carried out without regard to the period of stimulation.

2.2.2b Amplitude

Action potential amplitude decreases have been observed previously during chirps elicited in the Pn *in vivo* in *Eigenmannia* (Juranek and Metzner 1998) and in *A. leptorhynchus* (Dye and Heiligenberg 1987). Therefore the next parameter to be analysed *in vitro* was the post-stimulus action potential amplitude. Relative Pn action

potential amplitude is plotted for the first 10 cycles post-stimulation for the 50 and 500 μA stimuli (Figure 2.6). Only the first cycle after the 50 μA stimulus showed a significant difference in amplitude from the other cycles (One-way ANOVA on ranks and pairwise Tukey comparison, P=0.006), and this difference may have been due to small alterations in the amplitude caused by the electrical artifact of the stimulus (see Figure 2.3A immediately after the stimulus). The 500 μA stimulus however caused a significant decrease in amplitude across the first five post-stimulus cycles (One-way ANOVA on ranks and pairwise Tukey comparison, P<0.001). Amplitude changes do not appear to be related to cell type (data not shown), however more pacemaker cells than relay cells exhibited amplitude decreases post-stimulation. The larger number of pacemaker cell responses may have been partially the result of a sampling effect, since many more cells were identified by waveform as being pacemaker cells than relay cells (34 pacemaker vs. 11 relay cells).

2.2.2c Relative phase lag

To reveal the mechanism by which the Pn generates chirping, it is necessary to examine any changes that occur in the relationships between cells within the same nucleus. In Figure 2.7, the relative phase lag of 24 cell pairs for the first ten post-stimulus cycles is shown. The 50 μA stimulus elicited no change in the phase lag between cells in a pair post-stimulation (Figure 2.7A); one-way ANOVA on ranks, P=0.333. The 500 μA stimulus however (Figure 2.7B) caused a significant change in the phase lag for the first five cycles following stimulation (One-way ANOVA on ranks and pairwise Tukey test

P<0.01). An F-test of the phase responses comparing the phase lags of each of the first nine post-stimulus cycles to those of the tenth post-stimulus cycle revealed that this difference was largely due to an increase in variance (P<0.01). This same trend of increasing in variance post-stimulation was also evident in individual cell pairs (Figure 2.7C).

When changes in variability in the relative phase lag are separated according to cell type (results not shown), the results are similar to those observed in the population data (Figures 2.7A and 2.7B). Post-stimulus variability increased significantly for the first four cycles in pacemaker-relay cell pairings, and the first five cycles in pacemaker-pacemaker and relay-relay cell pairings (F-tests, P<0.01).

2.2.2d Glutamate pharmacology

Regulation of Pn activity occurs through inputs from the PPnC, PPnG and SPPn (Figure 1.1C). Inputs from PPnG and SPPn are NMDA-type and are responsible, respectively, for eliciting long-term frequency changes and the jamming avoidance response. Inputs from the PPnC are responsible for eliciting chirping, mediated by AMPA-type glutamate inputs present on the relay cells of the Pn (Juranek and Metzner 1998). By blocking PPnC inputs pharmacologically, it is possible to determine if the relative phase lag changes reported in the previous section may be involved in chirping.

In my experiments, NMDA receptor antagonist AP-5 (50 μM) did not significantly alter the relative phase lag response. The relative phase lags of the first five post-stimulus cycles after a 500 μA stimulus were significantly different from the

pre-stimulus mean (One-way ANOVA on ranks and pairwise Tukey test, P=0.001). This pattern was similar to the pattern observed in control ACSF conditions for the 500 μA stimulus, indicating that NMDA inputs from PPnG and SPPn are not likely responsible for eliciting changes in the relative phase lag.

Blocking AMPA-type inputs from the PPnC with CNQX (20 μM) all but eliminated the relative phase lag response. Post-stimulus changes in the relative phase lag after the application of CNQX were not significant when compared to pre-stimulus values (one-way ANOVA on ranks, P=0.453). This indicates that the post-stimulus phase lag changes observed previously are likely due to AMPA-type inputs from the PPnC, and can thus be attributed to a chirp-like response.

F-tests revealed variance levels similar to control ACSF conditions for the AP-5 treatment ($P<0.01$). In both control conditions and under AP-5 treatment, there was an increase in the phase lag variance over the first five post-stimulus cycles. The CNQX treatment variance however was similar to that of the 50 μA stimulus (P=0.01), and there was no increase in the phase lag variance after stimulation. Effects of the CNQX on the relative phase lag were partially washed out with untreated ACSF after 30 minutes (one-way ANOVA on ranks, P=0.022). This indicates that an increase in phase lag variance can be attributed to AMPA-type inputs from the PPnC, and not NMDA-type inputs from PPnG and SPPn.

2.3 Discussion

2.3.1 Overview

Chirps involve brief accelerations of the EOD frequency during social interactions in weakly electric fish, and are most likely implicated in communication between fish (Zupanc et al. 2006, Zupanc 2002, Hupé and Lewis 2008). The pacemaker (Pn), a network of ~150 electrically-coupled, intrinsically oscillating cells in the hindbrain is thought to be the final modulatory center in the brain responsible for modulating the EOD, and is consequently responsible for elicting chirping. The nature of the chemical inputs to the pacemaker nucleus has been examined (Dye 1989, Metzner 1993, Juranek and Metzner 1998), and chirp-like responses have been elicited in the pacemaker nucleus *in vitro* with electrical stimulation of afferents (Dye 1988). However the biophysical mechanism by which chirps are generated is as yet unclear. I have proposed two alternatives for how chirps are generated by the Pn:

- Synchronous change: PPn input affects all Pn cells, causing them to simultaneously increase their frequency, and thus causing a net frequency increase.

- Desynchronization: PPn input causes a fraction of Pn cells to transiently and randomly change their frequency, causing an apparent frequency increase across the network resulting from a loss of synchrony between cells.

There has been some support for the desynchronization mechanism of chirp production in the pacemaker nucleus, but the thorough quantification of Pn cell responses required to evaluate the validity of this mechanism has been lacking. I have sought to resolve this issue by performing a more robust quantification of Pn cell responses to electrical stimulation *in vitro*, with the ultimate goal of determining the primary mechanism of chirp generation in the Pn.

I have shown that a brief 500 μA positive current pulse applied across the axons leading to the Pn causes variable cycle duration decreases in single cells in the Pn (Figures 2.4 and 2.5), amplitude decreases in the action potentials of single cells in the Pn(Figure 2.6) and changes in phase lags between pairs of cells (both pacemaker and relay) (Figure 2.7).

Responses were similar in magnitude to those seen by Dye (1988), but I have performed a more thorough and systematic analysis. Instead of treating these changes as net amplitude and frequency changes, I have normalized post-stimulus responses of each trial to its pre-stimulus mean. By normalizing the responses in this manner, results are not masked by any variation in baseline values over experiments or over the time course of an experiment. Comparing the response parameters of each trial relative to their baseline values has revealed a number of interesting differences when compared to previous findings.

2.3.2 Quantification of chirp-like responses in Pn: Single cell responses

Significant amplitude decreases of up to ~20% were observed for the first five post-stimulus cycles (Figure 2.6). These decreases were similar to amplitude changes observed by Dye (1988), however he placed an emphasis on baseline voltage increases, a parameter that I did not measure, since my study was chiefly concerned with timing parameters. Although I did observe baseline voltage increases, these baseline changes were almost always coincident with amplitude decreases. Both the amplitude and baseline changes are likely due to the evoked synaptic conductance, though an examination of the ionic mechanisms behind these amplitude and baseline changes would be needed to determine their relationship. A thorough examination of these ionic mechanisms would require stopping the intrinsic oscillation of the Pn, which was not possible in the current study. Possibilities for stopping Pn oscillation will be discussed in the Future Directions chapter (Chapter 3).

Although membrane voltage amplitude changes result from stimulation, I believe frequency and phase changes to be the primary contributors to chirping in the Pn. Dye (1988) presented evidence that the phase at which stimulation occurs affects the degree of post-stimulation oscillation frequency increase. I demonstrated that there is very little effect of stimulus phase on the post-stimulus cycle duration (Figure 2.4). There may be a slight tendency towards the first post-stimulus cycle being most variable when the stimulus occurs just before the action potential rising phase ($0.8<\theta_s<1$), but this trend is not continued in subsequent cycles (Figure 2.4B).

Though it has previously been observed that frequency increases after stimulation of Pn afferents are dependent on the phase at which the stimulus occurs (Figure 5C in Dye 1988), this observation may have been largely due to low sample sizes. The phase dependency observed by Dye (1988) was determined using a single cell, whereas I have presented data for 45 cells. I did observe some trends towards phase dependency in individual cell pairs (Figure 2.5), but these trends were variable among cell pairs (data not shown). This variability resulted in a net effect of randomized cycle duration decreases across the cell population (Figure 2.4B).

2.3.3 Quantification of phase lags between paired cells

A single pacemaker nucleus was used by Dye (1988) to observe phase lags between paired cells. He noted that phase lags between cells were altered by Pn afferent stimulation (Figures 7B and 9B in Dye, 1988), and that these phase lag changes varied widely between trials. I have quantified this observation further, by investigating eight pacemaker nuclei, looking at post-stimulus phase lags between paired cells relative to their pre-stimulus baseline values (Figure 2.7). In my experiments the 500 μA stimulus caused a significant increase in the variance of phase lags between cells (Figure 2.7B). This post-stimulus increase in variance across cells is also mirrored by increases in variance within individual cell pairs (Figure 2.7C), in relay-pacemaker, relay-relay and pacemaker-pacemaker cell types (data not shown).

Dye (1988) observed cell type-dependent changes in cycle duration and phase, though he used a single Pn and only 24 individual trials, so the differential effects

observed may be a result of his low sample sizes. Histological identification of cell types combined with a robust quantification of phase lag changes would be needed to conclusively reveal any differences in relay and pacemaker cell phase responses. When cell types were identified by waveform, the phase lag responses in different cell type pairings to the 500 μA stimulus (data not shown) were similar to those observed in the overall population data (Figure 2.7B).

Selective pharmacological blockage of inputs from PPnG and PPnC confirmed that phase lag changes are due to PPnC input activation, and consequently phase lag changes are likely to be involved in the production of chirps in the Pn. AP-5 blocks NMDA-type inputs from PPnG and SPPn, whereas CNQX blocks AMPA-type input from PPnC (Figure 1.1C, Dye et al., 1989, Kawasaki and Heiligenberg, 1990, Zupanc and Maler, 1997, Zupanc, 2002, Juranek and Metzner, 1998). When AP-5 (50 μM) was applied to the Pn it had no effect on the phase lag response, but additional application of CNQX (20 μM) eliminated post-stimulus phase lag changes. The elimination of the post-stimulus phase lag changes with CNQX indicates that the transient desynchronization seen between Pn cells, as evidenced by increased phase lag variability post-stimulation (F-tests, $P<0.01$), may be a result of PPnC input activation. The question then arises: How can a desynchronization of Pn cell firing result in a chirp?

2.3.4 Creating chirps in the Pn: Desynchronization

Chirps can involve frequency excursions of upwards of 100 Hz, and occur over the space of only tens of milliseconds (Zupanc 2002, Zakon 2002, Hupé and Lewis, 2008). How does the Pn, a network of coupled oscillators firing in synchrony, create such a dramatic frequency change over such a short time scale? For the answer to this question, I have examined two options for the mechanism of chirp generation in the Pn: synchronous frequency changes and desynchronization. Synchronous frequency change is the most parsimonious solution, but desynchronization of a relatively weakly-coupled network of oscillators can also cause an overall frequency increase much greater than that of the individual oscillators (Indic et al., 2007, Mar et al., 1999).

Consider a generic neuronal oscillator with two populations of cells normally oscillating in sychrnony at the same frequency. If there is a pure synchronous frequency increase both populations simultaneously increase their frequency while maintaining stable phase lag relationships, causing an overall apparent frequency increase. If the coupling strength between cells in a neuronal oscillator is weak relative to the strength of the oscillation, the net activity of the entire population can be defined using the phases of sub-populations without considering amplitude (Indic et al. 2007). In other words, if the two sub-populations oscillate at the original frequency but exactly 0.5 cycles out of phase of one another, the apparent frequency of the entire population is doubled. Therefore if there is a pure desynchronization, neither population increases its oscillation frequency, but there is a temporary change in the phase lag relationships between the two, causing an apparent frequency change over the entire population.

Combining a synchronous frequency increase and desynchronization would allow for the greatest net frequency increase, because the two effects would be additive. For a visual description of each of the above scenarios, see Figure 2.8.

I have determined that a combination of synchronous change and desynchronization mechanisms is likely responsible for chirping, since it would allow for the greatest frequency increase at short latency. Driving EOD production is presumably energetically costly, which may account for the presence of a desynchronization mechanism. If raising the EOD frequency is a significant energetic cost, using a desynchronization mechanism would be one way to lower this cost while maintaining the ability to perform large frequency excursions. However, chirps are very brief (~15-30 ms), therefore an increased energetic cost would only be observed during extended bouts of chirping. Indeed, the energetic cost of increasing the EOD frequency at the whole animal level is also unclear (Moorhead, Perry, Lewis and Gilmour 2008, personal communication).

In addition to energetic advantages, the desynchronization mechanism takes advantage of the nature of the synaptic inputs to the Pn. Since chirping inputs from the PPnC synapse mostly onto the relay cells, the pacemaker cells would not be directly affected by these inputs (Kawasaki and Heiligenberg, 1990, Zupanc and Maler, 1997, Zupanc, 2002, Juranek and Metzner, 1998). Excitation of PPnC inputs increases the frequency of firing of relay cells but in a somewhat randomized fashion (Figures 2.4 and 2.7 and Dye, 1988), causing the oscillation of the relay cells to be desynchronized from each other and from the unaffected pacemaker cell population. If sub-populations of relay cells are activated briefly in a sequential fashion, frequency rises during

chirping would have a smooth onset and offset. The seemingly random arrangement of cells (Elekes and Szabo, 1985 and Figure 2.1) within the Pn would facilitate sequential activation assuming there is no structural time compensation for cells located further from the PPnC.

2.3.5 Generating chirps in the electric organ by desynchronization

Production of the EOD in *A. leptorhynchus* and other species has been modeled (Chapter 5 in Assad, 1997). Examining chirping within his EOD generation model, Assad demonstrated that the electrocytes must be activated sequentially in *A. leptorhynchus* to generate the wave-type EOD. He also proposed that the overall EOD amplitude decreases observed during chirping involve both desynchronous currents and individual sources of decreased amplitude. Since the response of Pn cells to brief stimulation is to transiently desynchronize (Figure 2.7), the output of the Pn during chirping may also be asynchronous. If EOD production is energetically costly to the electric organ, it may need to desynchronize to generate an elevated frequency, applying a concept similar to my proposed mechanism of chirp generation in the Pn (Figure 2.8). Receiving asynchronous input from the Pn could drive desynchronization of the electric organ cells and consequently would explain the decreased amplitude of the EOD observed during chirping (Assad, 1997, Dye, 1988).

Figure 2.1. Confocal micrographs of pacemaker nucleus tissue stained for fluorescence

Confocal micrographs of pacemaker nucleus tissue infused with neurobiotin via anterograde transport and labeled for fluorescence with streptavidin-CY3. Pacemaker cells (Pm), relay cells (Re) and parvocells (Pr) are shown in (A), showing numerous processes extending from and ending at each cell. In B, the intracellular space of a pacemaker cell (Pm) is shown filled with neurobiotin, whereas the intracellular space of the relay cell (Re) is not filled with neurobiotin. Synaptic boutons were observed as club-shaped protrusions at the periphery of pacemaker cells (C) and relay cells (D) whose locations are indicated with white arrows. Relay cells, pacemaker cells and parvocells shown are approximately 60-80 μm, 30-50 μm and 15 μm in diameter, respectively. Scale bars = 50 μm for A and B, 10 μm for C and D.

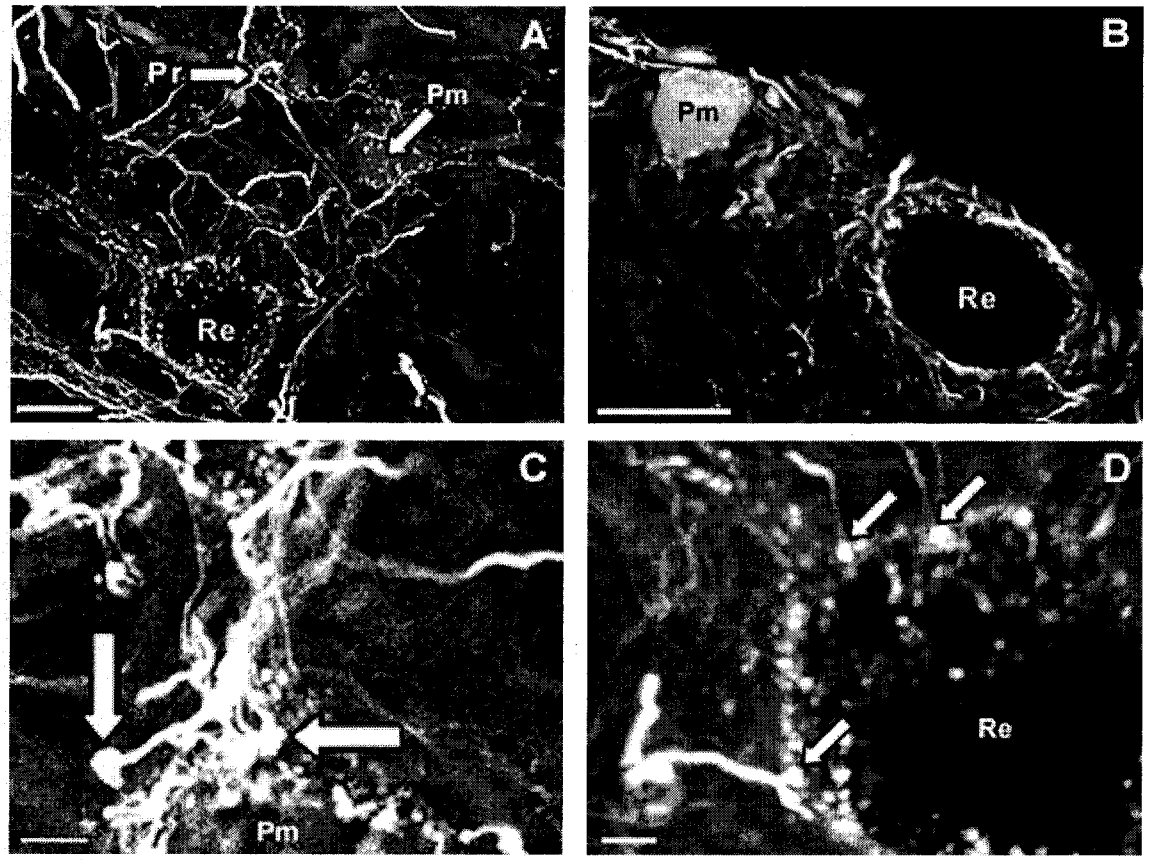
A
Pr
Pm
Re
B
Pm
Re
C
Pm
D
Re

Figure 2.2. Schematic diagram of the distribution of cell types in the pacemaker nucleus.

Schematic diagram of the distribution of cell types in the pacemaker nucleus. Counts from 150 μm serial sections are shown in (A), (B) and (C), with relay cells (large dots) and pacemaker cells (small dots). Insets show the approximate angle and width of each section from a rostrocaudal perspective, where the oval region is the pacemaker nucleus and the rectangular region is the surrounding brain tissue. The left side of the fish and corresponding side of the tissue section is indicated with an asterisk. Shown in (D) are total counts for pacemaker (Pm) and relay (Re) cells pooled over the three slices in (A) through (C), grouped into five regions from a dorsoventral perspective. Orientation and depth of the slices were taken into account when assigning cells to specific regions.

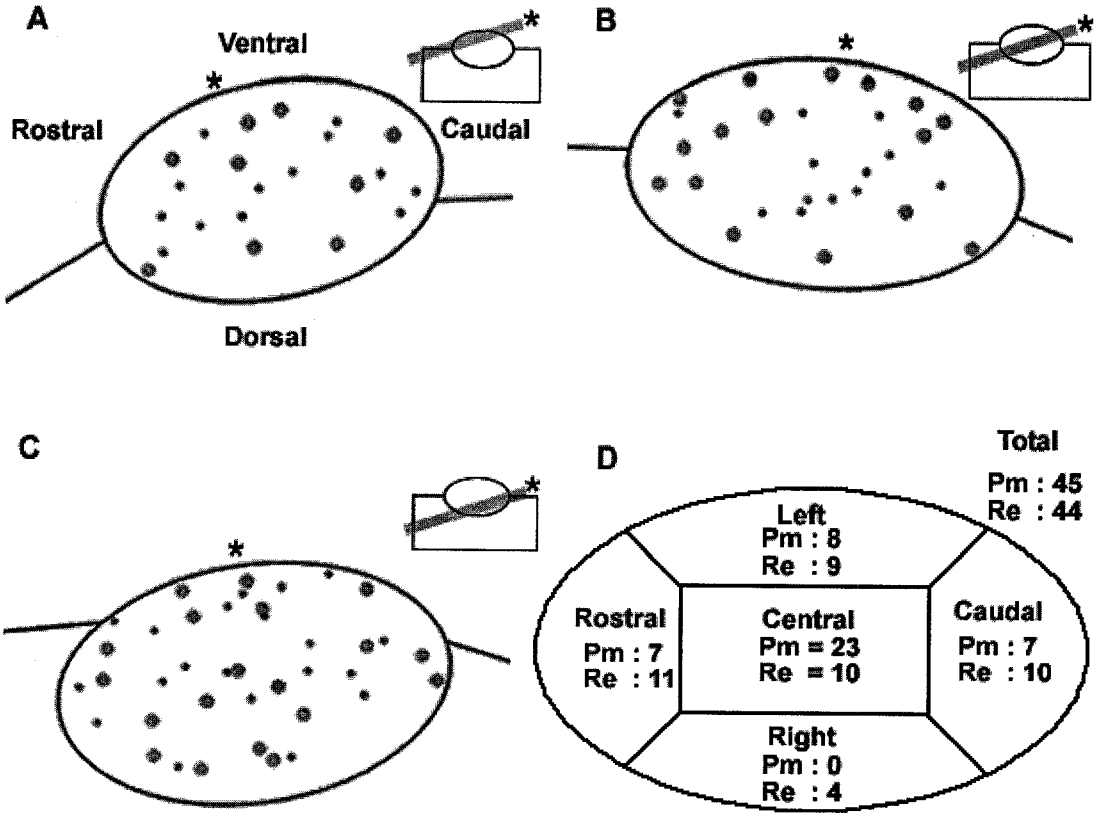
A
Ventral
Rostral
Caudal
Dorsal
B
C
D
Total
Pm : 45
Re : 44
Left
Pm : 8
Re : 9
Rostral
Pm : 7
Re : 11
Central
Pm = 23
Re = 10
Caudal
Pm : 7
Re : 10
Right
Pm : 0
Re : 4

Figure 2.3. Visual description of action potential amplitude, cycle duration and relative phase lag measurements.

Intracellular recordings from individual pacemaker nucleus cells (A and B), and traces from simultaneously recorded pacemaker (C, top trace) and relay cells (C, bottom trace). Panel A shows the method used for calculating relative amplitude (V_{rel}), whereas (B) shows the method used for calculating normalized post-stimulus cycle duration (T_x) and the phase of stimulation (θ_{stim}). V_{rel} and T_x are normalized to mean amplitude and cycle duration of the ten cycles immediately preceding the stimulus (V_{pre} and T_{pre}). The relative phase lag between pairs of recorded cells (φ_{rel}, calculation shown in panel C) was also normalized to the pre-stimulus phase lag (φ_{pre}) between each cell pair.

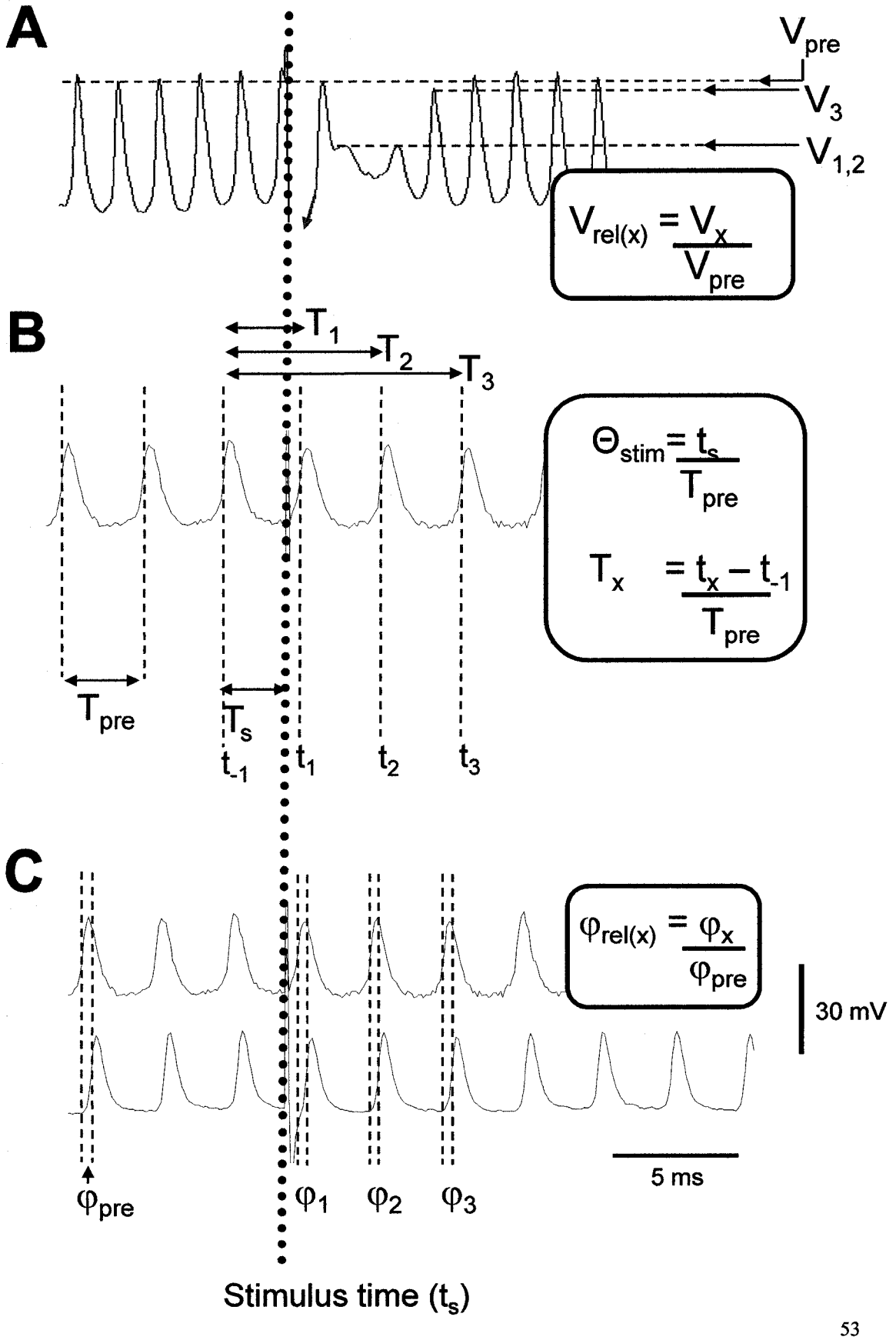
A
V_{pre}
V_3
$V_{1,2}$
$V_{rel(x)} = \frac{V_x}{V_{pre}}$
B
T_1
T_2
T_3
$\Theta_{stim} = \frac{t_s}{T_{pre}}$
$T_x = \frac{t_x - t_{-1}}{T_{pre}}$
T_{pre}
T_s
t_{-1}
t_1
t_2
t_3
C
$\varphi_{rel(x)} = \frac{\varphi_x}{\varphi_{pre}}$
30 mV
5 ms
φ_{pre}
φ_1
φ_2
φ_3
Stimulus time (t_s)

Figure 2.4. Phase response curves for first three post-stimulus cycles

Phase response curves for 50 μA (Panel A, control) and 500 μA (B and C) positive square-pulse current stimuli each lasting 100 μs. Normalized cycle periods for the first three post-stimulus cycles are shown. Note that the first cycle after the 500 μA stimulus (panel B) shows a slight tendency towards increased variation if the stimulus occurred later in the cycle, just before the positive zero-crossing. The second and third cycles after the 500 μA stimulus show increased variation throughout all stimulus phases (panel B). The phase response curves of ten trials from simultaneously recorded individual relay (filled circles) and pacemaker (empty circles) cells are shown in (C). Note that the responses of the two cells are similar in magnitude. (n=35 cells for Panel A, n=45 cells for Panel B)

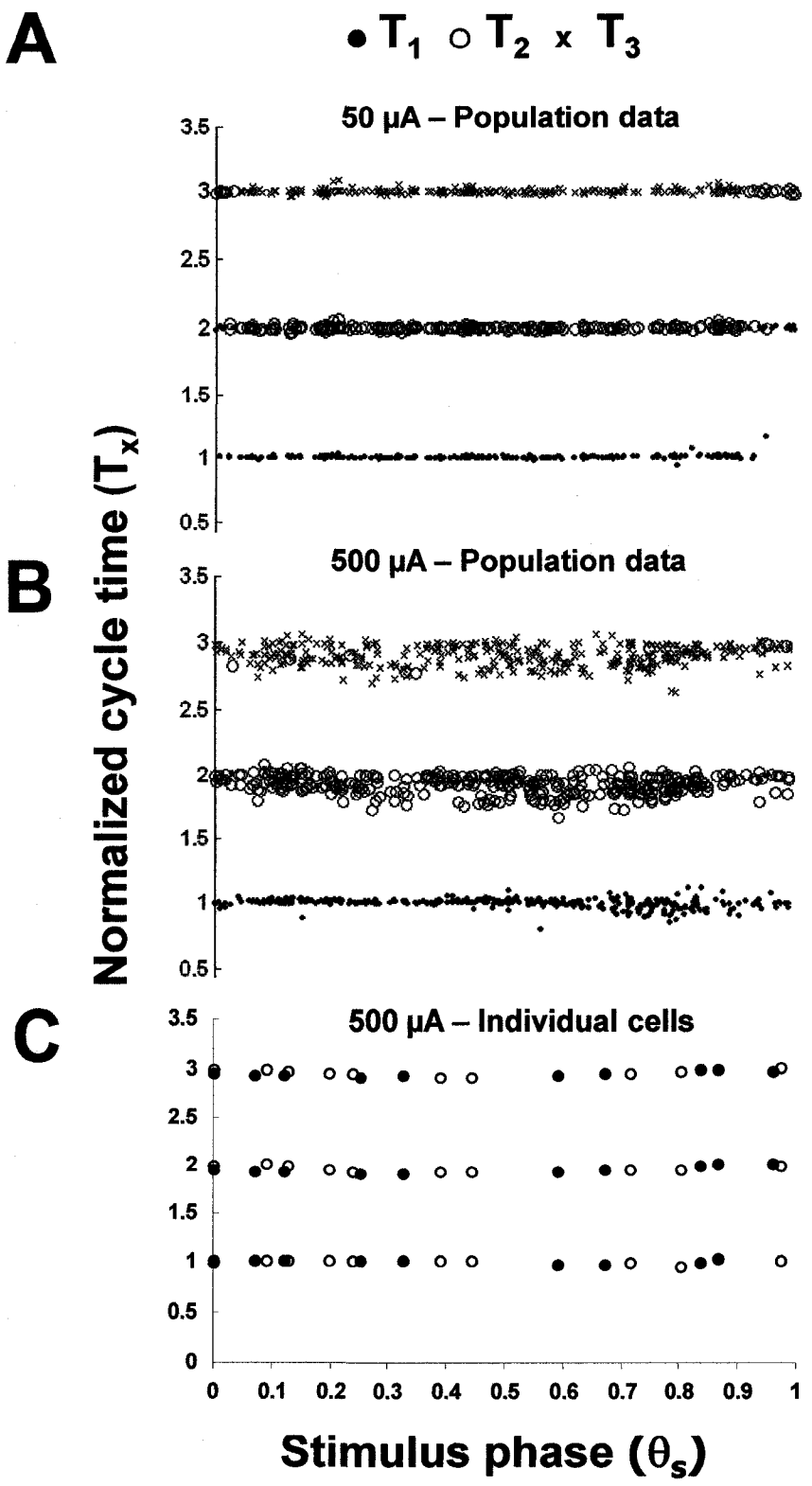
A
● T_1 ○ T_2 x T_3
50 µA – Population data
B
500 µA – Population data
C
500 µA – Individual cells
Normalized cycle time (T_x)
Stimulus phase (θ_s)
3.5
3
2.5
2
1.5
1
0.5
0
0 0.1 0.2 0.3 0.4 0.5 0.6 0.7 0.8 0.9 1

Figure 2.5. Phase response curves for first three post-stimulus cycles in an individual cell pair.

Phase response curves for 500 μA positive square-pulse current stimuli each lasting 100 μs in a single pacemaker-relay cell pair over ten trials. Normalized cycle periods for the first three post-stimulus cycles are shown for an individual cell pair consisting of a simultaneously recorded relay cell (filled circles) and pacemaker cell (empty circles). Datum from the same cell pair presented in Figure 2.4C are presented here, with a smaller scale to clarify trends. The first cycle post-stimulation is represented in (T_1, A), whereas the second and third cycles are presented in (T_2, B) and (T_3, C) respectively. Note that the normalized cycle duration values for (B) and (C) are similar, indicating that there was little change in the cycle duration between the second and third post-stimulus cycles. It should also be noted that the greatest discrepancies between the responses of the two cell types occurs when the stimulus occurs immediately before or immediately after the zero-crossing ($0<\theta_s<0.2$ and $0.9<\theta_s<1$) in cycles 2 and 3 (B and C). For cycle 1 (A) the trend is similar to the population data presented in Figure 2.7B, with the largest cycle duration changes occurring immediately before the zero-crossing ($0.7<\theta_s<1$).

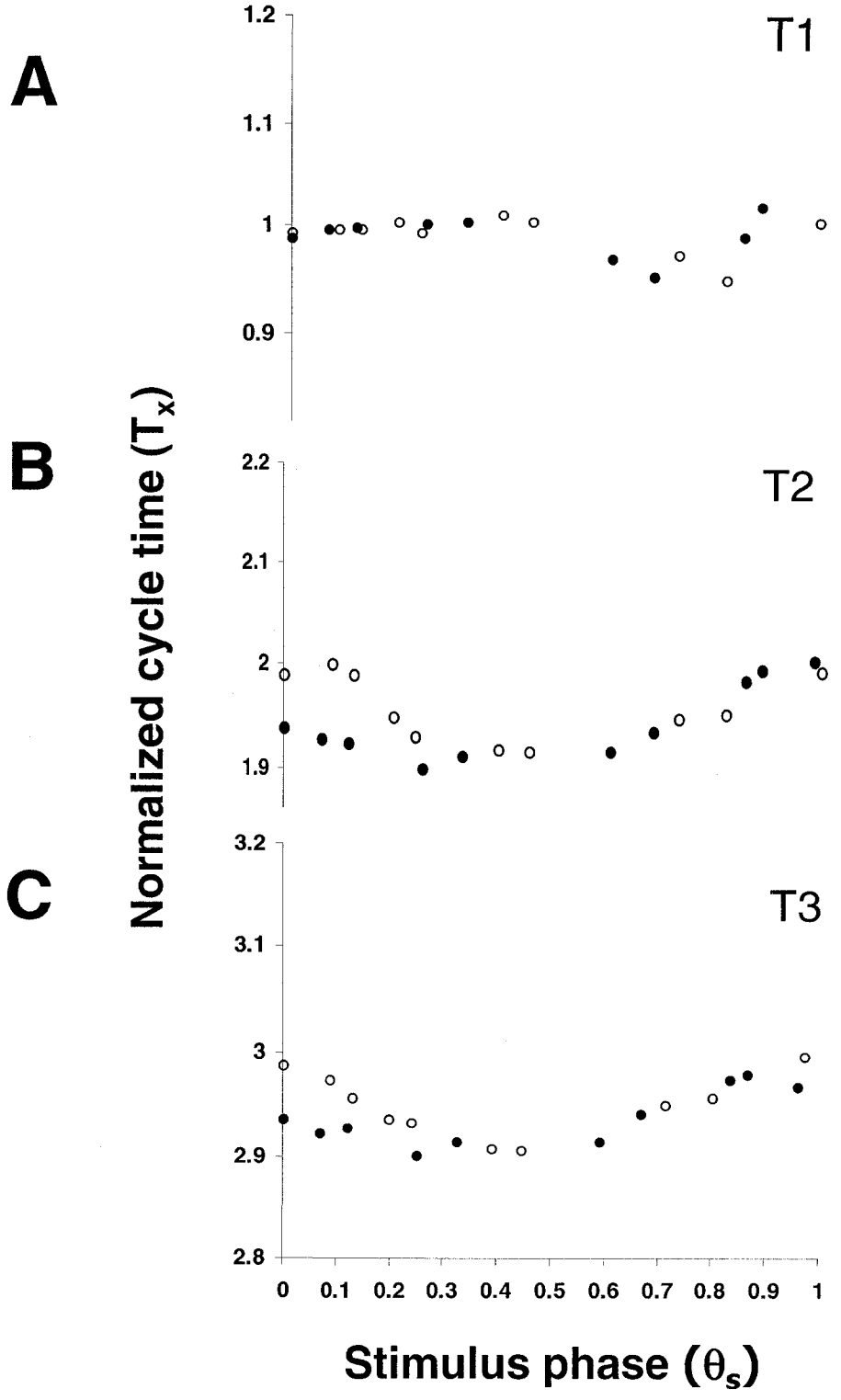
A
B
C
T1
T2
T3
1.2
1.1
1
0.9
2.2
2.1
2
1.9
3.2
3.1
3
2.9
2.8
0
0.1
0.2
0.3
0.4
0.5
0.6
0.7
0.8
0.9
1
Normalized cycle time (T_x)
Stimulus phase (θ_s)

Figure 2.6. Relative amplitude of first ten post-stimulus cycles

Relative amplitude (V_{rel}) of the first ten post-stimulus cycles for 50 μA (Panel A) and 500 μA (B) positive square-pulse stimuli each lasting 100 μs. The mean is indicated with a solid black line ± SD (dashed line). A one-way ANOVA on ranks revealed a significant difference in the amplitude across cycles for the 500 μA stimulus (Panel B, $P<0.001$). There was also a significant difference between the first post-stimulus cycle and most subsequent cycles with the 50 μA stimulus (Panel A, one-way ANOVA on ranks, $P=0.006$), however this difference may be attributable to an electrical artifact from the stimulus. N = 20 cells (202 trials) for the 50 μA stimulus; 28 cells (352 trials) for the 500 μA stimulus.

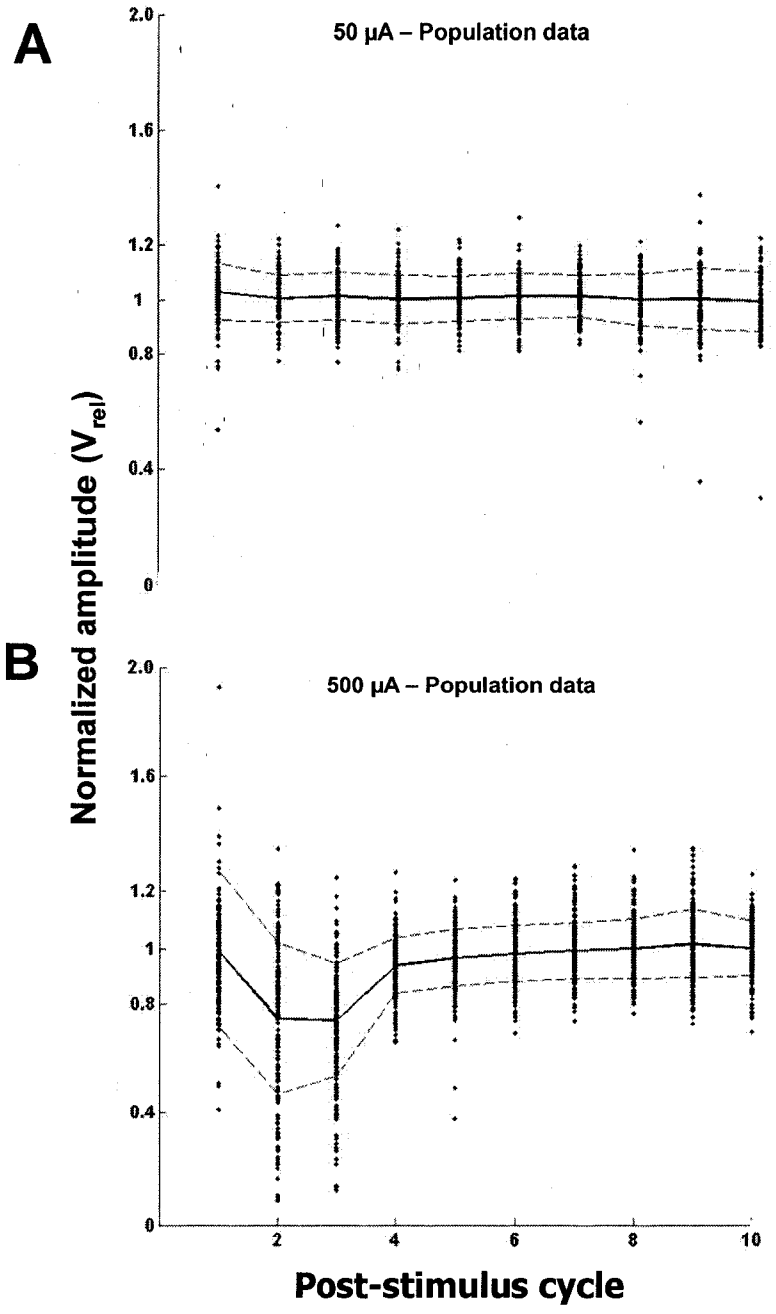
A
50 µA – Population data
B
500 µA – Population data
Normalized amplitude (V_{rel})
Post-stimulus cycle
2.0
1.6
1.2
1
0.8
0.4
0
2
4
6
8
10

Figure 2.7. Relative phase lag of first ten post-stimulus cycles

Relative phase lag (φ_{rel}) of the first ten post-stimulus cycles for 50 μA (Panel A) and 500 μA (B and C) positive square-pulse stimuli each lasting 100 μs. Pre-stimulus relative phase lag had a mean value of 0.16±0.32 for the 500 μA stimulus. Panels A and B represent population data for all cell pairs, whereas Panel C represents data from a single pacemaker-pacemaker cell pair. The mean is indicated with a solid black line ± SD (dashed line). A one-way ANOVA on ranks revealed a significant difference across cycles for the 500 μA stimulus population data (Panel B, $P<0.001$), but not for the 50 μA stimulus (Panel A, $P=0.333$). An F-test on the variance of the 500 μA population data was performed, in which the variance of the first nine post-stimulus cycles was compared to that of the tenth. The variances of cycles 1 to 5 were significantly different than control (F-test, $P<0.01$), as indicated with asterisks (*) in Panel B. It should be noted that this variance is due both to variance between cell pairs in the population (B), it is also due to variance within individual cell pairs, as exemplified in (C). (n=20 cell pairs, 65 trials for Panel A, n=24 cell pairs, 158 trials for Panel B)

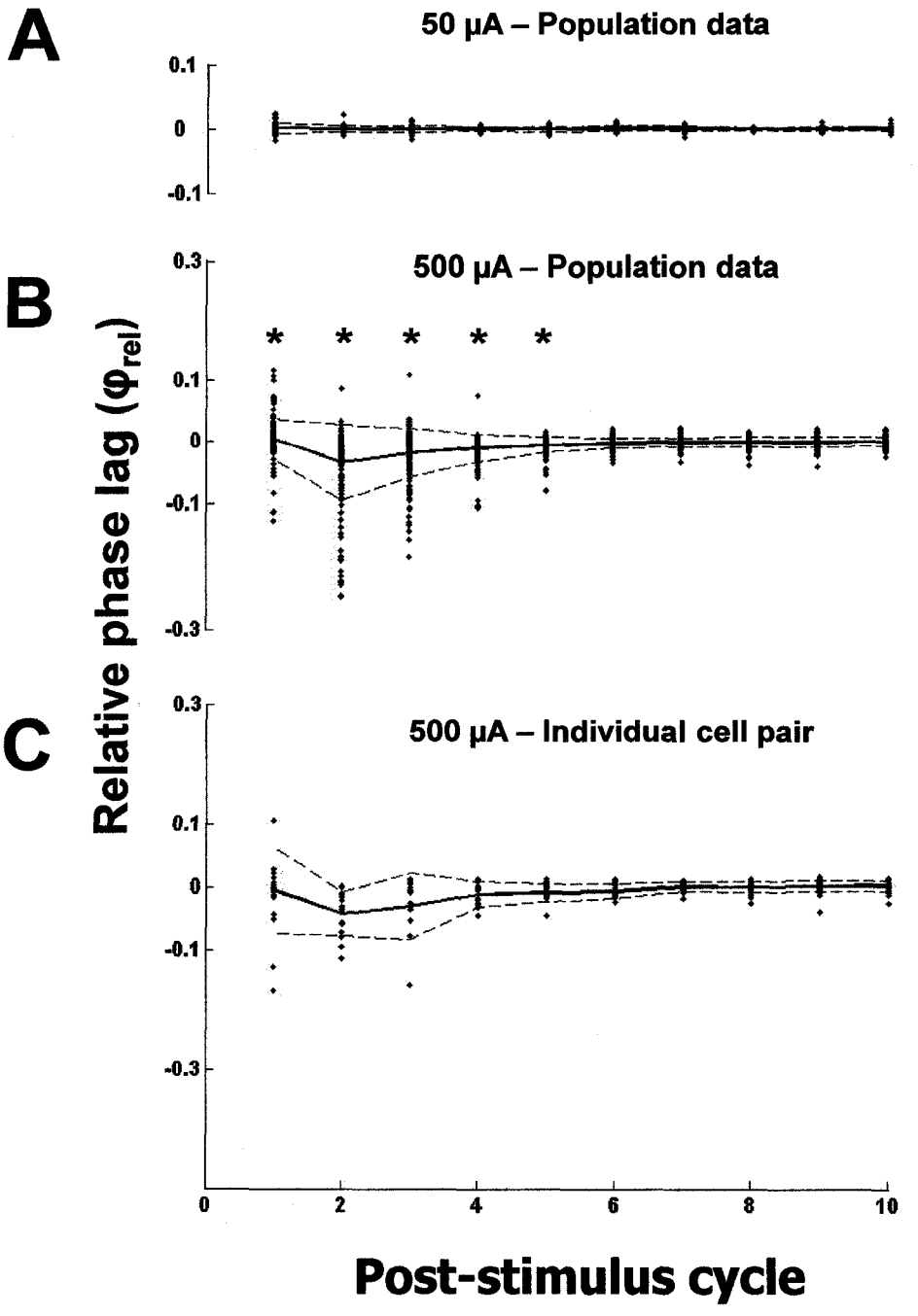
A
50 µA – Population data
0.1
0
-0.1
B
500 µA – Population data
0.3
0.1
0
-0.1
-0.3
* * * * *
C
500 µA – Individual cell pair
0.3
0.1
0
-0.1
-0.3
Relative phase lag (φ_{rel})
0
2
4
6
8
10
Post-stimulus cycle

Figure 2.8. Visual description of chirp-generation mechanisms in the pacemaker nucleus

Schematic of the creation of chirping in the pacemaker nucleus (Pn) through frequency increases and desynchronization, based on the phase-splitting modeling of an idealized network of coupled oscillators (Indic et al. 2007). In each panel a simulated Pn cell population voltage trace (solid line) is shown with zero-crossing times indicated below it as dashed lines ending in filled dots to represent net frequency change over the entire population of Pn cells. Dotted lines represent a second population of Pn cells oscillating out of phase of the population represented by the solid line. (A) Undisturbed Pn in which all cells are oscillating in synchrony at baseline frequency F_0. (B) Pn post-stimulation in which all cells are oscillating in synchrony at an increased frequency F_1. (C) Pn post-stimulation in which two populations of cells are oscillating at the baseline frequency F_0, but at a non-zero relative phase lag (φ_{rel}). This causes an overall frequency ($F_{population}$) greater than that of F_0, and similar to that observed by a synchronous frequency increase as observed in (B). The greatest overall frequency increase is achieved in (D) by increasing the oscillation frequency of cells similarly to (B), and combining it with a phase shift similarly to (C).

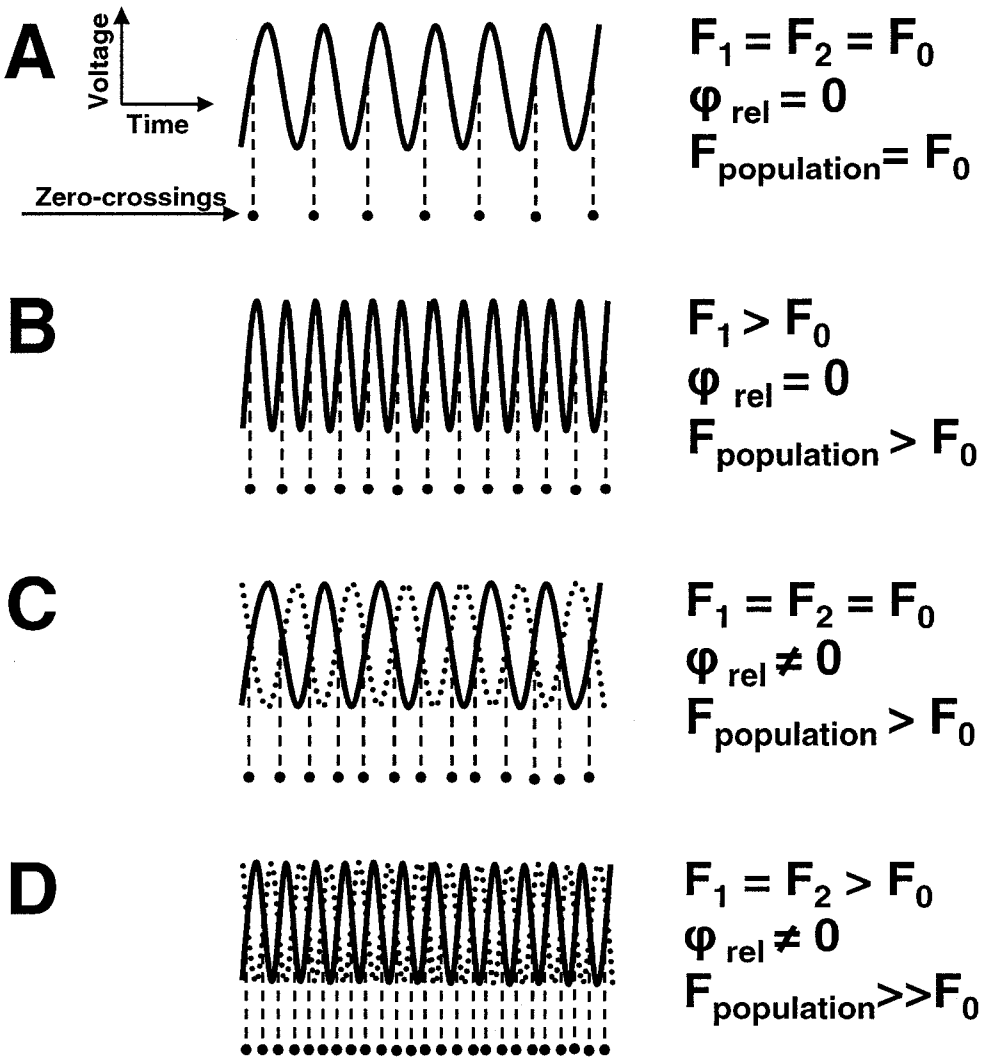
A
Voltage
Time
Zero-crossings
$F_1 = F_2 = F_0$
$\varphi_{rel} = 0$
$F_{population} = F_0$
B
$F_1 > F_0$
$\varphi_{rel} = 0$
$F_{population} > F_0$
C
$F_1 = F_2 = F_0$
$\varphi_{rel} \neq 0$
$F_{population} > F_0$
D
$F_1 = F_2 > F_0$
$\varphi_{rel} \neq 0$
$F_{population} >> F_0$

Chapter 3

Conclusions and Future Directions

3.1 General conclusions

I have quantified chirp-like responses elicited in the Pn by applying single 500 μA current pulses across Pn afferents and recording from Pn cells *in vitro*. This stimulus evoked action potential amplitude decreases and somewhat randomized decreases in cycle duration in single cells. It also induced changes in the phase lag between pairs of simultaneously recorded cells, which were accompanied by an increase in variation in the phase lag. Post-stimulus phase lag changes became non-significant with the application of CNQX but not AP-5, indicating that phase lag changes are likely due to chirp-inducing inputs from the PPnC. The somewhat randomized nature of the post-stimulus cycle duration decreases and phase lag changes suggest that a desynchronization of the oscillation of Pn cells occurs during chirping. The degree of randomization of the post-stimulus phase lag and cycle duration changes implicate desynchronization as the primary mechanism for chirp generation in the Pn.

3.2 Synaptic mechanisms of Pn cell responses

To study the synaptic mechanisms of amplitude reduction and baseline changes in Pn cells, it would be necessary to stop the intrinsic oscillation of the Pn. It would also be necessary to use an agent that would not prevent synaptic responses, such as something that would block the action of one or more ionic channels involved in the Pn cell responses to stimulation.

One possibility I investigated is the use of the gap-junction blocker Carbenoxolone (CLX). Without the current and resistive load from surrounding cells, it is possible that Pn cells would not be able to continue oscillating. CLX concentrations of approximately 1 mM in bath application have been shown to successfully stop Pn oscillation (Moortgat et al., 2000b). However, when I bath-applied CLX at 0.5 and 1 mM concentrations, the Pn did not cease to oscillate (one Pn used per concentration, data not presented). Further experimentation would be required to conclusively determine the effectiveness of CLX in stopping Pn oscillation, and whether it also has any effects on post-stimulus changes in relative phase lag.

Another approach is to directly inhibit Pn cells through pharmacological activation of inhibitory synapses. GABA is a common vertebrate inhibitory neurotransmitter, so I used GABA agonists in an attempt to induce an increase in cycle duration of oscillation in Pn cells. GABA receptor agonists Muscimol ($GABA_A$, 20 μM) and Baclofen ($GABA_B$, 25 μM) did not succeed in stopping oscillation in the Pn after 20 minutes of application. The overall amplitude of the oscillation was slightly attenuated, but the cycle duration remained stable over the entire duration of the application (data not presented).

Since the cycle duration of the EOD is known to be negatively proportional to temperature (Q_{10}=1.65 from Smith and Zakon, 2000, Q_{10}=1.21 from Julie Warrington, unpublished observations), two experiments were conducted in which the Pn was cooled to try to drive the cycle duration to higher values. If the oscillation frequency is driven sufficiently low, it may be possible to measure the synaptic effects of stimulation of Pn afferents without interference from the intrinsic oscillation. Small ice cubes made

from control ACSF were placed inside the brain slice chamber with the Pn so that the ACSF flowing over and around the Pn would be as close to the melting point as possible without damaging the Pn through direct contact with the ice. This method resulted in a frequency drop of ~100 Hz, which equates to a ~25% frequency drop in most of my Pn preparations (data not presented). Cooling did not attenuate the frequency enough to be able to observe synaptic effects of stimulation. It is possible that though cooling does reduce the frequency of oscillation in the Pn, oscillation in the Pn is resistant to large changes in its oscillation frequency due to both the extensive nature of the coupling between cells and the thickness of the tissue slice (~500 μm). It may be necessary to more carefully control the temperature and cool the Pn for a much longer period of time (hours) to observe a larger effect.

Altering the ionic concentrations of the ACSF to achieve a low Mg^{2+} ACSF has been shown to successfully induce seizure-like rhythmic activity in rat hippocampal preparations (Tancredi et al., 1990, Albus et al., 2008), and high Mg^{2+}, low Ca^{2+} saline has been shown to inhibit bursting activity in rat spinal slice culture (Ballerini et al., 1999), and to slow the frequency of Pn firing *in vitro* in *A. leptorhynchus* (Dye et al. 1989). Therefore, I applied high Mg^{+2} (20 mM) ACSF to two pacemaker nuclei in separate experiments for 60 minutes each in an attempt to inhibit rhythmic activity in the Pn. In one of the two experiments, the ACSF was also Ca^{+2}-free. The change in ionic concentration did not cause the Pn to stop oscillating, nor did it have a noticeable effect on the baseline amplitude or frequency or post-stimulation response. Other avenues along the same lines that could be explored would be to eliminate Mg^{+2} from

the ACSF, further increase the Mg^{+2} concentration, or inject a high-concentration Mg^{+2} ACSF directly into Pn cells.

Though some of the methods used to attempt to stop Pn oscillation had small effects, none of these methods successfully stopped the oscillation of the Pn. One avenue that was not explored was the possibility of recording from the Pn immediately after it is removed from the brain. Similarly to previous studies (Spiro, 1997), the Pn slice was given 60-120 minutes of recovery time in which the Pn was allowed to recover its intrinsic oscillation to a suitable level of stability as determined by qualitative observation of the cycle duration of action potential oscillations. I made one attempt to record from a Pn during its recovery, but within 30 minutes of the dissection some of the cells had begun to oscillate at over 100 Hz (data not presented). I was unable to determine whether responses to stimulation at that point were consistent with responses observed after the recovery period, due to the poor signal to noise ratio resulting from low action potential amplitude.

It may be necessary to use some of the methods I outlined above that had some effect on the Pn oscillation (CLX, cold ACSF, GABA agonists) during the recovery to achieve a long recording period free of intrinsic oscillations. Though when used in isolation none of the methods I described were successful in my experiments, their subtle effects may, either alone or in combination, be enough to prevent the Pn from recovering its oscillatory activity immediately post-dissection.

3.3 Characterization of the reponses of Pn cell types

Dye (1988) noted differences in the responses of pacemaker and relay cells to short current pulses. Attempts were made to identify cells by waveform in my experiments, but in many cases (17 out of 45 total cells) cells were not conclusively identified as either pacemaker or relay cells. It is likely that in cases where no distinction could be made between cell types that those cells were pacemaker cells, since the number of pacemaker cells far outweighs that of relay cells (Elekes and Szabo, 1985, Moortgat et al. 2000). To conclusively identify individual electrode penetration sites, it may be necessary to shorten the number of trials per cell and only record from 1-2 cells in a given Pn. This approach would minimize dye coupling resulting from Neurobiotin leakage during long recordings. If multiple cells from a single Pn are iontophoresed, they should be as far apart as possible to facilitate identification even if some dye coupling occurs.

Juranek and Metzner (1998) characterized the segregation of pharmacological inputs to Pn in *Eigenmannia*, but a similar quantification is lacking for the Pn of *A. leptorhynchus*. Additionally, though they determined that inputs from PPnG lead to pacemaker cells, and those from PPnC lead to relay cells (Figure 1.1C), the relative changes in input resistance were not observed exclusively in one cell type when each pre-pacemaker nucleus was stimulated (Figure 8 in Juranek and Metzner, 1998). Input resistance changes were observed in relay cells during glutamate stimulation of PPnG, and similarly changes were observed in pacemaker cells upon stimulation of PPnC. The lack of all-or-none changes in input resistance in the two cell types suggests that the

representation of exclusive inputs from either PPnC or PPnG to the different cell types (Figure 1.1C) may not be entirely accurate.

The synapses from PPnC and PPnG may not exclusively extend to either relay or pacemaker cells, and instead there may simply be more inputs of one type to each. Alternately, there may be some feedback inputs from the relay cells to pacemaker cells, which could indirectly affect the timing of pacemaker cell oscillations. Either scenario would explain why in my study pacemaker-pacemaker cell pairings showed changes in phase lags post-stimulation, but phase lag changes were eliminated with the application of AMPA-type glutamate receptor blocker CNQX. If there was no influence (direct or indirect) of AMPA-type inputs to the Pn on the pacemaker cells, it would be expected that CNQX would have not been effective in eliminating the phase lag response.

The third cell type found in the Pn, parvocells, have largely been disregarded in the study of functioning of the Pn. It has been shown that parvocells connect to both relay and pacemaker cells, and are found throughout the Pn (Smith et al., 2000). Their role in Pn oscillation and its behavioral responses has not yet been examined. I believe that parvocells may play an important supportive role in Pn function, either to maintain stability, facilitate behavioral changes or a combination of both. Since inhibition-coupled networks have reduced noise (Mar et al., 1999), if the parvocells are inhibitory they may function to stabilize the oscillation of the Pn by reducing noise.

3.4 Characterizing relay cell output

One of the important next steps in studying chirping *in vitro* is to determine if the desynchronization observed when stimulating the Pn carries through to create asynchronous output by the relay cells. If this asynchronous output then causes the firing of electric organ cells to be temporarily desynchronized as well, it could account for the characteristic amplitude decrease and frequency increase observed during chirping (Assad 1997, and see Figure 2.8 for explanation). Combining a net increase in the oscillation frequency of the Pn (Figure 2.8B) with a change in the phase lag between cell populations (Figure 2.8C) would result in the additive effect of a relatively high increase in the net frequency of oscillation of Pn cells (Figure 2.8D). An increase in Pn cell oscillation would cause an increase in the number action potentials received by electric organ cells from the relay cells, causing an increase in the EOD frequency. Similarly, a desynchronization of those action potentials may cause the electric organ cells to fire asynchronously, causing the characteristic amplitude decreases seen during chirping (Zupanc 2002, Zakon et al. 2002, Hupé and Lewis 2008).

Before making electrophysiological recordings from relay cell axons, it would be necessary to carry out anterograde labeling from relay cell bodies to determine the exact location of relay cell axons within the spinal cord. After determining the path taken by the relay cell axons to reach the electric organ, it will then be possible to modify the *in vitro* Pn preparation. Modifications would seek to incorporate a longer section of spinal cord and do electrophysiological recordings in the relay cell axons. Ideally, similar Pn stimulation and recording protocols to those used by Dye (1988) and

myself could be implemented simultaneously with recordings of relay cell axons to determine the extent to which desynchronization extends past the level of the Pn.

3.5 Chirping in the Pn *in vivo*

Ultimately, to test of the desynchronization mechanism it will be necessary to record from Pn cells in live fish. Using methods similar to *in vivo* preparations previously described (Dye et al. 1989, Kawasaki and Heiligenberg, 1990, Juranek and Metzner, 1997), but extending them to include simultaneous recording from multiple Pn cells would reveal whether the Pn does indeed desynchronize during chirping. *In vivo* preparations could also be used to record from the relay cell axons, or Pn cells and relay cell axons simultaneously.

Appendix

Glossary of terms

Apteronotus leptorhynchus	South American species of weakly electric fish; brown ghost knifefish
ACSF	Artificial cerebrospinal fluid; solution used to bathe brain preparations during *in vitro* experiments to maintain tissu health
AFR	Abrupt frequency rise; category of brief communication signal used by *A. leptorhynchus* during aggressive encounters
AMPA	alpha-amino-3-hydroxy-5-methyl-4-isoxazolepropionic acid; glutamate receptor agonist specific to AMPA-type glutamate receptors
anterograde labelling	Neuronal labeling procedure in which a substance is transported to a region of interest through its efferent axons
AP-5	(2*R*)-amino-5-phosphonopentanoate; NMDA-type glutamate receptor antagonist
Baclofen	GABA-B Receptor agonist
biological oscillator	Organs, tissues or cells that exhibit rhythmic activity in living systems
bipolar stimulation	Stimulation of neural tissue across a tract of axons efferent to a region of interest
brown ghost knifefish	See *A. leptorhynchus*
chirp	Short (~15 ms) communication signal used by wave-type weakly electric fish during social interactions; Chirps involve characteristic frequency increases and amplitude decreases
CLX	Carbenoxolone; gap junction blocker
CNQX	6-cyano-7-nitroquinoxaline-2,3-dione; AMPA/kainate-type glutamate receptor antagonist
CV	Coefficient of variation = Standard deviation / Mean cycle duration
desynchronization mechanism	Mechanism for the generation of chirping in the pacemaker nucleus that involves a transient randomization of the phase and frequency of individual pacemaker nucleus cells
electric organ	Organ common to electric fish; generates an electric field used primarily in navigation and communication
electric organ discharge (EOD)	Electric field generated by the electric organ; used in weakly electric fish for navigation and communication
electrophysiology	Study of the electrical properties of cells and tissues
electrosensory system	System of specialized skin receptors and associated neural structures designed to detect and interpret external electric signals
ELL	Electrosensory lateral line lobe; part of the brain of weakly electric fish responsible for initial processing of electrosensory information
GABA	Gamma-aminobutyric acid; inhibitory neurotransmitter

glutamate	Excitatory neurotransmitter
immunohistochemistry	Process of localization of proteins in tissue using specific antibodies and antigens; often involves attaching fluorescent probes to antibodies
in vitro	Experiment performed on living tissue removed from an organism
intracellular recording	Electrical recordings inside a cell, typically performed with sharp borosilicate glass or quartz electrodes
intrinsic oscillator	Oscillator that does not need input from an outside source to maintain its oscillation
JAR	Jamming avoidance response; Response in wave-type weakly electric fish in which fish in close proximity with similar EOD frequencies alter their EOD frequency so the two frequencies do not "jam" each other
LTFE	Long-term frequency elevation; Long-term (seconds to hours) elevation of the EOD frequency of a weakly electric fish; can be induced naturally or experimentally through repeated (tetanic) stimulation
MS-222	Tricane Methanosulfate; anaesthetic
Muscimol	GABA-A receptor agonist
nE	Nucleus electrosensorius; neural control structure in the electrosensory system of weakly electric fish
neurobiotin	Tracer protein used for immunohistochemistry of neurons
NMDA	N-methyl-D-aspartic acid; glutamate receptor agonist specific to NMDA-type glutamate receptors
nP	Nucleus praeeminentialis; neural structure that is part of the electrosensory processing feedback pathway in the brain of weakly electric fish
pacemaker cell	Cell type found in the pacemaker nucleus of wave-type electric fish; receives NMDA-type synaptic input from SPPn and PPnG
pacemaker nucleus (Pn)	Brainstem neural structure in weakly electric fish that contains intrinsically-oscillating electrically coupled cells
parvocell	Interneuron found in the pacemaker nucleus of weakly electric fish
phase lag	Relative phase lag of oscillation of two coupled oscillators; Calculated using the timing of a cycle in one oscillator relative to the other, and dividing the timing difference by the mean cycle duration of the two oscillators
phase response curve (PRC)	Plot of the cycle duration of an oscillation relative to the phase at which a perturbation to the oscillator occurred

PPnC	Segment of the PPn responsible for eliciting chirping
PPnG	Segment of the PPn responsible for eliciting long-term frequency changes
prepacemaker nucleus (PPn)	Descending neural control structure in the brain of weakly electric fish
pulse-type EOD	Electric organ discharge that is emitted as discrete pulses of electricity
relay cell	Cell type found in the pacemaker nucleus of wave-type electric fish; receives AMPA-type synaptic input from PPnC; the axons of relay cells synapse onto the cells of the electric organ
SAN	Sinoatrial node; structure in the heart of vertebrates responsible for regulating the heartbeat
SCN	Suprachiasmatic nucleus; structure in the brain of vertebrates responsible for regulating the circadian day/night rhythm
SPPn	Sublemniscal prepacemaker nucleus; Descending control structure in the brain of weakly electric fish responsible for eliciting the jamming avoidance response
synchronous change mechanism	Mechanism for the generation of chirping in the pacemaker nucleus that involves a synchronous increase in the frequency of all cells in the pacemaker nucleus
wave-type EOD	Electric organ discharge that is emitted as a continuous wave-like discharge of electricity
weakly electric fish	Fish that emit a weakly electric field using their electric organ

Bibliography

Albus, K., Wahab, A., and Heinemann, U. (2008). Standard antiepileptic drugs fail to block epileptiform activity in rat organotypic hippocampal slice cultures. Br J Pharmacol *154*, 709-24.

Alves-Gomes, J.A., Orti, G., Haygood, M., Heiligenberg, W., and Meyer, A. (1995). Phylogenetic analysis of the South American electric fishes (order Gymnotiformes) and the evolution of their electrogenic system: a synthesis based on morphology, electrophysiology, and mitochondrial sequence data. Mol Biol Evol *12*, 298-318.

Assad, C. (1997). Electric field maps and boundary element simulations of electrolocation in weakly electric fish. PhD thesis submitted to the University of Ottawa .

Ballerini, L., Galante, M., Grandolfo, M., and Nistri, A. (1999). Generation of rhythmic patterns of activity by ventral interneurones in rat organotypic spinal slice culture. J Physiol *517 (Pt 2)*, 459-75.

Barbuti, A., Baruscotti, M., and Difrancesco, D. (2007). The pacemaker current: from basics to the clinics. J Cardiovasc Electrophysiol 18, 342-347. 2007.

Bastian, J., Chacron, M.J., and Maler, L. (2004). Plastic and nonplastic pyramidal cells perform unique roles in a network capable of adaptive redundancy reduction. Neuron *41*, 767-79.

Caputi, A.A. (2004). Contributions of electric fish to the understanding of sensory processing by reafferent systems. J Physiol Paris *98*, 81-97.

Caputi, A.A. and Budelli, R. (2006). Peripheral electrosensory imaging by weakly electric fish. J Comp Physiol A Neuroethol Sens Neural Behav Physiol *192*, 587-600.

Curti, S., Comas, V., Rivero, C., and Borde, M. (2006). Analysis of behavior-related excitatory inputs to a central pacemaker nucleus in a weakly electric fish. Neuroscience 140, 491-504.

Curti, S., Falconi, A., Morales, F.R., and Borde, M. (1999). Mauthner cell-initiated electromotor behavior is mediated via NMDA and metabotropic glutamatergic receptors on medullary pacemaker neurons in a gymnotid fish. J Neurosci 19[20], 9133-9140.

Dye, J. (1988)An in vitro physiological preparation of a vertebrate communicatory

behavior: chirping in the weakly electric fish, *Apteronotus*. J Comp Physiol A 163, 445-458.

Dye, J. and Heiligenberg, W. (1987). Intracellular recording in the medullary pacemaker nucleus of the weakly electric fish, *Apteronotus*, during modulatory behaviors. J Comp Physiol A 161, 187-200.

Dye, J., Heiligenberg, W., Keller, C.H., and Kawasaki, M. (1989). Different classes of glutamate receptors mediate distinct behaviors in a single brainstem nucleus. Proc Natl cad Sci 86, 8993-8997.

Edwards, J.G. and Michel, W.C. (2003). Pharmacological characterization of ionotropic glutamate receptors in the zebrafish olfactory bulb. Neuroscience *122*, 1037-47.

Elekes, K. and Szabo, T. (1985). Synaptology of the medullary command (pacemaker) nucleus of the weakly electric fish (*Apteronotus leptorhynchus*) with particular reference to comparative aspects. Exp Brain Res 60, 509-520.

Ellis, D.B. and Szabo, T. (1980). Identification of different cell types in the command (pacemaker) nucleus of several gymnotiform species by retrograde transport of horseradish peroxidase. Neuroscience 5, 1917-1929.

Engler, G. and Zupanc, G.K. (2001). Differential production of chirping behavior evoked by electrical stimulation of the weakly electric fish, *Apteronotus leptorhynchus*. J Comp Physiol [A] *187*, 747-56.

Fortune, E.S. (2006). The decoding of electrosensory systems. Curr Opin Neurobiol *16*, 474-80.

Friesen, W.O. and Block, G.D. (1984). What is a biological oscillator? Am J Physiol Regulatory Integrative Comp Physiol 246, 847-853.

Glass and Mackey (1988). From Clocks to Chaos: The Rhythms of Life. (Princeton, New Jersey: Princeton University Press).

Heiligenberg, W., Metzner, W., Wong, C.J. and Keller, C.H. (1996). Motor control of the jamming avoidance response of Apteronotus leptorhynchus: evolutionary changes of a behavior and its neuronal substrates. J Comp Physiol [A] 179(5):653-674.

Hopkins, C.D. (1995). Convergent designs for electrogenesis and electroreception. Current Opinion in Neurobiology *5*, 769-777.

Hupé, G.J. and Lewis, J.E. (2008). Electrocommunication signals in free swimming

brown ghost knifefish, Apteronotus leptorhynchus. J Exp Biol *211*, 1657-67.

Ijspeert, A.J. (2008). Central pattern generators for locomotion control in animals and robots: A review. Neural Netw *21*, 642-53.

Indic, P., Schwartz, W.J., and Paydarfar, D. (2007). Design principles for phase-splitting behaviour of coupled cellular oscillators: clues from hamsters with 'split' circadian rhythms. J R Soc Interface. 5[25]:873:883.

Jonkers, F.C., Jonas, J.-C., Gilon, P., and Henquin, J.-C. Influence of cell number on the characteristics and synchrony of Ca^{+2} oscillations in clusters of mouse pancreatic islet cells. J Physiol 520[3], 839-849. 1999.

Juranek, J. and Metzner, W. (1997). Cellular characterization of synaptic modulations of a neuronal oscillator in electric fish. J Comp Physiol A 181, 393-414.

Juranek, J. and Metzner, W. (1998). Segregation of behavior-specific synaptic inputs to a vertebrate neuronal oscillator. J Neurosci 18[21], 9010-9019.

Kalsbeek, A., Kreier, F., Fliers, E., Sauerwein, H.P., Romijn, J.A., and Buijs, R.M. (2007). Minireview: Circadian control of metabolism by the suprachiasmatic nuclei. Endocrinology *148*, 5635-9.

Kang, H., Jo, J., Kim, H.J., Choi, M.Y., Rhee, S.W., and Koh, D.S. (2005). Glucose metabolism and oscillatory behavior of pancreatic islets. Phys Rev E Stat Nonlin Soft Matter Phys *72*, 051905.

Karnup, S. and Stelzer, A. (2001). Seizure-like activity in the disinhibited CA1 minislice of adult guinea-pigs. J Physiol *532*, 713-30.

Kawasaki, M. and Heiligenberg, W. (1990). Different classes of glutamate receptors and gaba mediate distinct modulations of a neuronal oscillator, the medullary pacemaker of a gymnotiform electric fish. J Neurosci 10[12], 3896-3904.

Kelly, M., Babineau, D., Longtin, A., and Lewis, J.E. (2008). Electric field interactions in pairs of electric fish: modeling and mimicking naturalistic inputs. Biol Cybern *98*, 479-90.

Lissmann, H.W. (1951). Continuous electrical signals from the tail of a fish. *Gymnarchus niloticus Cuv.* Nature *167*, 201-2.

Lissmann, H.W. and Machin, K.E. (1958). The mechanism of object location in *Gymnarchus niloticus* and similar fish. J Exp Biol 35,451-486 (1958) 35, 451-486.

Mathieson, W.B. and Maler, L. (1988). Morphological and electrophysiological properties of a novel in vitro preparation: the electrosensory lateral line lobe brain slice. J. Comp. Physiol. [A]. 163(4): 489-506.

Mar, D.J., Chow, C.C., Gerstner, W., Adams, R.W., and Collins, J.J. (1999). Noise shaping in populations of coupled model neurons. Proc Natl Acad Sci U S A *96*, 10450-5.

McCrea, D.A. and Rybak, I.A. (2008). Organization of mammalian locomotor rhythm and pattern generation. Brain Res Rev *57*, 134-46.

Mears, D., Sheppard, N.F., Atwater, I., and Rojas, E. (1995). Magnitude and modulation of Pancreatic B-cell gap junction electrical conductance *In situ*. J Membrane Biol 146, 163-176.

Metzner, W. (1993). The jamming avoidance response in Eigenmannia is controlled by two separate motor pathways. J Neurosci *13*, 1862-78.

Meyer, J.H. Steroid influences upon discharge frequencies of intact and isolated pacemakers of weakly electric fish. J Comp Physiol A 154, 659-668. 1984.

Mileva, G., Zysman, D., and Lewis, J. (2008). *In vitro* studies of closed-loop feedback and electrosensory processing in *Apteronotus leptorhynchus*. J Physiol [Paris].

Moore, R.Y. (2007). Suprachiasmatic nucleus in sleep-wake regulation. Sleep Med *8 Suppl 3*, 27-33.

Moortgat, K.T., Bullock, T.H., and Sejnowski, T.J. (2000a) Precision of the pacemaker nucleus in a weakly electric fish: network versus cellular influences. J Neurophysiol 83, 971-983.

Moortgat, K.T., Bullock, T.H., and Senjowski, T.J. (2000b). Gap junction effects on precision and frequency of a model pacemaker network. J Neurophysiol 83, 984-997.

Moortgat, K.T., Keller, C.H., Bullock, T.H., and Sejnowski, T.J. (1998). Submicrosecond pacemaker precision is behaviorally modulated: the gymnotiform electromotor pathway. Proc Natl Acad Sci 95, 4684-4689.

Oestreich, J. and Zakon, H.H. (2002). The long-term resetting of a brainstem pacemakern ucleus by synaptic input: a model for sensorimotor adaptation. J Neurosci 22[18], 8287-8296.

Rose, G.J. (2004). Insights into neural mechanisms and evolution of behaviour from

electric fish. Nat Rev Neurosci *5*, 943-51.

Smith, G.T. (1999). Ionic currents that contribute to a sexually dimorphic communication signal in weakly electric fish. J Comp Physiol A 185, 379-387.

Smith, G.T. (2006). Pharmacological characterization of ionic currents that regulate high-frequency spontaneous activity of electromotor neurons in the weakly electric fish, Apteronotus leptorhynchus. J Neurobiol *66*, 1-18.

Smith, G.T., Lu, Y., and Zakon, H.H. (2000). Parvocells: a novel interneuron type in the pacemaker nucleus of a weakly electric fish. J Comp Neurol 423, 427-439.

Smith, G.T. and Zakon, H.H. (2000). Pharmacological characterization of ionic currents that regulat the pacemaker rhythm in a weakly electric fish. J Neurobiol 66[1], 1-18.

Spiro, J.E. (1997). Differential activation of glutamate receptor subtypes on a single class of cells enables a neural oscillator to produce distinct behaviors. J Neurophysiol 78, 835-847.

Tancredi, V., Hwa, G.G., Zona, C., Brancati, A., and Avoli, M. (1990). Low magnesium epileptogenesis in the rat hippocampal slice: electrophysiological and pharmacological features. Brain Res *511*, 280-90.

Triefenbach, F. and Zakon, H. (2003). Effects of sex, sensitivity and status on cue recognition in the weakly electric fish *Apteronotus leptorhynchus*. Animal Behaviour 65, 19-28.

Zhang, Y. and Han, V.Z. (2007). Physiology of morphologically identified cells in the posterior caudal lobe of the mormyrid cerebellum. J Neurophysiol 98, 1297-1308. 2007.

Zupanc, G.K., Sirbulescu, R.F., Nichols, A., and Ilies, I. (2006). Electric interactions through chirping behavior in the weakly electric fish, Apteronotus leptorhynchus. J Comp Physiol A Neuroethol Sens Neural Behav Physiol *192*, 159-73.

Zupanc, G.K.H. (2002). From oscillators to modulators: behavioral and neural contro lof modulations of the electric organ discharge in the gymnotiform fish, *Apteronotus leptorhynchus*. J Physiol Paris 96, 459-472. Zupanc, G.K.H. and Heiligenberg, W. (1992). The structure of the diencephalic prepacemaker nucleus revisited: light microscopic and ultrastructural studies. J Comp Neurol 323, 558-569.

Zupanc, G.K.H. and Maler, L. (1997). Neuronal control of behavioral plasticity: the prepacemaker nucleus of weakly electric fish. J Comp Physiol A 180, 99-111.